Development of immunotherapy using antigen-loaded multifunctional small extracellular vesicles

2021

LIU WEN

Preface

Extracellular vesicles (EVs) are released by cells of almost all types of living organism including human, animal, plant, and microorganism. Release of EVs have a wide range of significant physiological consequences[1–4]. Small EVs of membrane blebs were first identified as being produced by maturing reticulocytes[5]. Since then, research has progressed gradually, and in 2007, it was reported that EVs can deliver mRNAs and miRNAs that they carry, which has led to a significant development in EV research[6].

As researchers study EVs more intensively, more and more subpopulations of EVs were discovered[7]. According to minimal information for studies of extracellular vesicles 2018 (MISEV2018) guidelines published by international society of extracellular vesicles[8], EV subtypes can be differentiated by their physical characteristics such as size (small EVs: < 100nm or < 200nm, or large EVs and/or medium EVs: > 200nm). Particularly, small EVs (sEVs), also called as exosomes in the earlier studies, enclose endogenous proteins and nucleic acids derived from their cells of origin and play important roles as carriers in cell−cell communication by delivering enclosed cargo to recipient cells[9,10]. Because of their intrinsic nature as endogenous delivery carriers, sEVs are considered as a novel and promising candidate of drug delivery system (DDS).

There are many other lipid-based nano-sized delivery systems such as liposomes, which have a lengthy and well-studied history in drug delivery research[11,12]. Compared to liposomes, sEVs contain endogenous biological molecules (RNAs and antigens). Moreover, exogenous antigens or functional molecules can be loaded to sEVs by genetic engineering to enable preparation of multifunctional sEVs [13]. These unique properties of sEVs would be the rationale for the development of antigen-loaded multifunctional sEV-based immunotherapy.

For immunotherapeutic application of sEV, antigen loading, delivery to immune cells (especially dendritic cells (DCs) and activation of the immune cells are important factors. In this thesis, I investigated the effect of modifying endogenous antigen-containing sEVs with CD40L, a peptide ligand with DCs-directing and immunostimulatory properties. Moreover, to create more types of multifunctional sEVs, I explored the possibility of loading exogenous antigens onto the sEVs. Since the exogenous antigens can be loaded onto the outside or inside of the lipid bilayer of sEVs, I investigated the effects of antigen localization on the efficiency of antigen presentation by sEVs-engulfed immune cells. After optimizing the loading method

of exogenous antigens, I attempted to construct multifunctional sEVs by modifying the adjuvant to the antigen-loaded sEVs and evaluated the possibility of using it to treat allergic rhinitis.

Table of Contents

Chapter 1

Development of endogenous antigen containing multifunctional sEVs for effective induction of anti-tumor immune response

I-1 Introduction

Tumor-derived small extracellular vesicles (sEVs), which contain endogenous tumor antigens, are anticipated to be used as a source of tumor antigens to induce tumor antigen-specific immune responses without the requirement for the identification of a particular tumor antigen[14–16].

In inducing anti-tumor immune response by using endogenous tumor antigens containing sEVs, they need to be taken up by dendritic cells (DCs), which are antigen presenting cells. DCs can then process and load tumor antigens on to MHC class I molecules for presentation to $CD8^+$ T cells through the process known as cross presentation[17]. The efficiency of cross presentation can be significantly enhanced by targeting antigens to receptors expressed on the DCs[18]. These receptors include c-type lectins (e.g., DEC205, LOX-1), as well as non-lectin receptors such as CD40, mannose receptor, and integrins. It has been demonstrated that targeting CD40 is more efficient than targeting lectin receptors such as DEC205 and LOX-1 in the induction of antigen-specific $CD8^+$ T cell responses[19,20].

CD40, a costimulatory protein, is a member of the tumor necrosis factor (TNF)-receptor superfamily. CD40 was initially found on the surface of B lymphocytes and was subsequently found to be expressed on the surface of monocytes, endothelial cells, and DCs. The CD40 ligand (CD40L), also known as CD154, belongs to the TNF superfamily and was first identified on activated $CD4^+$ T cells[21]. CD40L can bind to CD40 expressed on DCs and activate them into fully competent antigen-presentation cells. CD40-CD40L interaction has been shown to play an important role in the induction of $CD8^+$ T-cell immunity by DCs through IL-12 production and antigen presentation to $CD8^+$ T-cells[22]. It was also reported that antigens taken up by DCs via CD40-mediated endocytosis tend to be retained in the early endosome, so that antigens are prevented from rapid degradation by the lysosome. The antigens taken up via CD40-mediated endocytosis are efficiently transported into the cytosol for proteasomal degradation and MHC class I presentation due to minimal degradation in the lysosome[23].

In this chapter, tumor cells-derived sEVs were modified with CD40L (CD40L-sEVs) for the effective induction of tumor-specific immune responses. It was hypothesized that tumor cells-derived sEVs modified with CD40L were targeted to the early endosome of DCs and the modified sEVs can generate a powerful stimulatory signal to activate DCs through CD40-CD40L interactions. Murine melanoma B16BL6 tumor cells were used as model sEVs-producing cells and B16BL6-derived sEVs were modified with CD40L-LA, a fusion protein of CD40L and sEV tropic protein lactadherin (LA). To investigate whether CD40L modification

can target DCs and activate them, the uptake and intracellular fate of CD40L-sEVs by DCs were evaluated. The amount of cytokines such as IL-12 and TNF-α released from the DCs and the expression of CD80 on the surface of DCs with sEVs were also evaluated. An antigen presentation assay was performed in order to estimate the antigen presentation ability of DCs with CD40L-sEVs.

I-2 Materials & Methods

Mice and cells.

Eight-week-old male C57BL/6 mice were purchased from Japan SLC, Inc. (Shizuoka, Japan). Protocols for all animal experiments were approved by the Animal Experimentation Committee of the Graduate School of Pharmaceutical Sciences, Kyoto University. Murine melanoma B16BL6 cells were obtained from the Riken BRC (Tsukuba, Japan) and cultured in Dulbecco's modified Eagle's medium (DMEM; Nissui Co., Ltd., Tokyo, Japan) containing 10 % fetal bovine serum (FBS) and 0.2 g/L of glucose. Mouse dendritic DC2.4 cells were kindly provided by Dr. K. L. Rock (University of Massachusetts Medical School) and cultured in 10 % FBS-containing RPMI 1640 (Nissui Co., Ltd., Tokyo, Japan), supplemented with 0.5 mM monothioglycerol and 0.5 mM non-essential amino acids. A mouse colon carcinoma cell line (colon-26) was obtained from the Cancer Chemotherapy Center of the Japanese Foundation for Cancer Research (Tokyo, Japan) and cultured in 10 % FBS-containing RPMI 1640 (Nissui Co., Ltd., Tokyo, Japan). BUSA14 cells (murine T cell hybridoma cells specific for melanoma antigen gp100) were a generous gift from Prof. L. Eisenbach (Weizmann Institute of Science, Rehovot, Israel) and cultured in 10 % FBS-containing RPMI 1640 (Nissui Co., Ltd., Tokyo, Japan), supplemented with 0.5 mM monothioglycerol and 0.5 mM non-essential amino acids[24]. Mouse T-cell hybridoma CD8-OVA1.3 cells, generously gifted by Dr. C. V. Harding (Case Western Reserve University), were cultured in complete 10% FBS-containing DMEM, supplemented with 0.5 mM monothioglycerol and 0.1 mM nonessential amino acids.

Construction of plasmid DNA (pDNA).

The coding sequence of LA was obtained as described in a previous report[25]. CD40L and FLAG coding sequences were synthetized by Fasmac Co., Ltd (Atsugi-shi, Kanagawa, Japan). The chimeric sequence of CD40L-LA with FLAG tag in the C-terminal fragment of LA was prepared by using the 2-step PCR method. Information regarding the primers used to synthesize the fusion proteins used in this study will be made available upon request. The

CD40L-LA-FLAG encoding fusion protein was inserted into the BamHI/Xbal site of the pcDNA3.1 vector (Thermo Fisher Scientific) to construct pCMV-CD40L-LA.

Collection of sEVs.

B16BL6 cells were transfected with the pCMV-CD40L-LA plasmid vector using PEI Max (Polysciences, Inc., Warrington, PA, USA) as described previously[26]. The supernatants of non-transfected and transfected cells were processed by sequential centrifugation (300 *g*, 10 min; 2,000 *g*, 20 min; 10,000 *g*, 30 min) followed by filtration through 0.2-μm syringe filters. The filtered sample was then ultracentrifuged for 1 h at 100,000 *g*. The sedimented sEVs pellets were washed twice in phosphate buffered saline (PBS) and were resuspended in PBS. The sEVs amounts were estimated by measuring the protein concentrations using Bradford assay. The TEVs used in this study have been characterized previously[27]. 1 μg of TEV proteins contain approximately 109 TEV particles.

Western blot.

After four freezing-and-thawing cycles, B16BL6 cell lysates were prepared by centrifugation at 15,000 *g* for 15 min to remove cell debris. The reduced sEVs or cell lysate samples (5 μg of protein) were loaded onto a 10% sodium dodecyl sulfate–polyacrylamide gel, and subject to sodium dodecyl sulfate polyacrylamide gel electrophoresis (SDS-PAGE) and then transferred to polyvinylidene fluoride transfer membranes (Merck Millipore Corporation, Billerica, MA, USA). After blocking using the Blocking One reagent (Nacalai Tesque, Kyoto, Japan), the membranes were incubated with the following primary antibodies at 4 ℃ overnight: mouse anti-Alix antibody (1:200; Santa Cruz Biotechnology), rabbit anti-HSP70 antibody (1:1000; Cell Signaling Technology, Danvers, MA, USA), rabbit anti-CD81 antibody (1:200; Santa Cruz Biotechnology, Dallas, TX, USA), rabbit anti-Calnexin antibody (1:1000; Santa Cruz Biotechnology), rabbit anti-Pmel17 (also was known as gp100) antibody (1:200; Santa Cruz Biotechnology) and mouse anti-FLAG M2 monoclonal antibody (1:1000; Sigma-Aldrich, USA), respectively. Then, the membranes were incubated with horseradish peroxidase (HRP)-conjugated rabbit anti-mouse IgG antibody (1:2000 dilution; Thermo Fisher, Waltham, MA, U.S.A.) or goat anti-rabbit IgG antibody (1:5000 dilution; Santa Cruz Biotechnology) for 1 h at 25 ℃. The membranes were reacted with Immobilon Western Chemiluminescent HRP substrate (Merck Millipore), and chemiluminescence was detected using the LAS-3000 instrument (FUJIFILM, Tokyo, Japan).

Transmission electron microscopy and particle size distribution of sEVs.

sEVs were treated with an equal volume of 4% paraformaldehyde (Nacalai Tesque, Kyoto, Japan) in PBS. The treated samples were then applied to a transmission electron microscope (TEM)-grid film coated with Carbon/Formvar (Alliance Biosystems, Osaka, Japan) and incubated at 25 ℃ for 20 min. The samples were fixed with 1 % glutaraldehyde for 5 min after washing with PBS. They were then stained with 1 % uranyl acetate for 5 min after being washed thrice in distilled water. The samples were observed using TEM (Hitachi H-7650; Hitachi High-Technologies). The particle size distribution of samples was evaluated by analyzing the obtained TEM images by ImageJ (Wayne Rasband National Institutes of Health, USA).

Zeta potential of sEVs.

sEVs (1 μg of protein) were mixed with distilled water. The suspension was added to a disposable folded capillary cell and a Zetasizer Nano ZS (Malvern Instruments, Malvern, U.K.) was used to determine the zeta potential of the sEVs.

Fluorescent labeling of sEVs.

The PKH67 green fluorescent cell linker kit was purchased from Sigma-Aldrich (St. Louis, MO, USA). The sEVs were resuspended in 200 μL of Diluent C and then treated with an equal volume of 2 μM PKH dye-containing Diluent C. The mixture was incubated for 5 min at 25 ℃. After stopping the reaction with 400 μL of 5 % bovine serum albumin (BSA)-containing PBS for 1 min at 25 ℃, the fluorescently labeled sEVs were ultracentrifuged at 100,000 *g* for 1 h for washing and were resuspended in PBS.

Cellular uptake of sEVs by cells.

DC2.4 cells and Colon-26 cells seeded in 96-well-plates at a density of 5.0×10^4 cells/well were cultured for 24 h at 37 ℃. PKH67-labeled sEVs were then added to the cells and incubated for 1, 2, 3, 4, 5, and 6 h at 37 ℃ and 4 ℃, respectively. The cells were then washed in PBS thrice and suspended in PBS. The cellular uptake of sEVs was evaluated by the Gallios Flow Cytometer (Beckman Coulter, Brea, CA, USA), according to the manufacturer's instructions. Data were analyzed using the Kaluza software (Beckman Coulter). The mean fluorescent intensity (MFI) was calculated as an indicator of cellular uptake.

Confocal Microscopy.

DC2.4 cells were seeded onto glass coverslips at a density of 1.5 × 10^4 cells/well and incubated for 24 h. The culture medium was replaced with fresh medium and then sEVs labeled with GFP were added to the cells. After 4 h of addition of sEVs, the cells were washed with PBS and fixed with 4% paraformaldehyde for 20 min. The samples were then incubated for 10 min with PBS containing 0.25% Triton X-100 (Nacalai Tesque, Kyoto, Japan). After washing with PBS for 5 min, the cells were incubated with 1% BSA and 22.52 mg/mL of glycine in PBST (PBS+ 0.1% Tween 20) for 30 min to block unspecific binding of the antibodies. The cells were then incubated in the diluted first antibody (anti-EEA1 antibody, 1:300, Abcam) in 1% BSA in PBST at 4°C overnight. Then the cells were incubated with the secondary antibody (Goat Anti-Rabbit IgG H&L (Alexa Fluor647), 1:1000, Abcam) in 1% BSA for 1 h at room temperature in the dark. Finally, 300 nM 4′,6′-diamidino-2-phenylindole (DAPI) was added and the cells were incubated for 5 min. After washing with PBS, the coverslips were mounted using SlowFade Gold (Thermo Fisher Scientific) to prevent fluorescent fading. The prepared samples were observed using a confocal microscope (A1R MP, Nikon Instech Co., Ltd., Tokyo, Japan). The pictures were analyzed by NIS-elements (Nikon Instech Co., Ltd., Tokyo, Japan).

Collection of bone marrow-derived dendritic cells (BMDCs).

To determine the antigen presentation capacity of sEVs, I collected BMDCs as described previously[28]. Briefly, bone marrow cells were isolated from C57BL/6 mouse femurs and tibias and were filtered through a 40 μm cell strainer (BD Falcon, Franklin Lakes, NJ) to eliminate bone and debris. After filtration, bone marrow cells were suspended in 0.86 % ammonium chloride for 1 min to lyse erythrocytes; the remaining cells were cultured for 6 days in complete 10 % FBS-containing RPMI 1640, supplemented with 20 ng/mL recombinant murine GM-CSF (Peprotech, Rocky Hill, NJ). The culture medium was changed every 2 days. Finally, non-adherent cells were harvested and used as BMDCs.

Cytokine release from BMDCs.

The BMDCs were seeded in a 96-well culture plate at a density of 5 × 10^4 cells/well. After 24 h incubation at 37 ℃, sEVs suspended in Opti-MEM were added to each well. BMDCs treated with 1 ng/mL lipopolysaccharide (LPS, Sigma-Aldrich St. Louis, MO, U.S.A.) and Opti-MEM were alone employed as positive and negative controls, respectively. After incubation at 37 ℃ for 8 h, the culture medium was centrifuged at 300 *g* for 3 min to collect

supernatants. The concentrations of tumor necrosis factor (TNF)-α and IL-12 in the supernatant were evaluated by the mouse TNF-α and mouse IL-12p40 enzyme-linked immunosorbent assay (ELISA) OptEIATM sets (Pharmingen, San Diego, CA, USA) according to the manufacturer's instructions.

Flow cytometry analysis of CD80 expressed on the surface of BMDCs.

The BMDCs were seeded in a 96-well culture plate at a density of 5×10^4 cells/well. After 24 h incubation at 37 ℃, sEVs suspended in Opti-MEM were added to each well. BMDCs treated with 1 ng/mL lipopolysaccharide (LPS, Sigma-Aldrich St. Louis, MO, U.S.A.) and Opti-MEM alone were employed as positive and negative controls, respectively. After incubation at 37 ℃ for 24 h, the BMDCs were washed twice in PBS and then collected. The BMDCs were incubated with the PE anti-mouse CD80 antibody (1:80 dilution; BioLegend, San Diego, CA.) for 20 min. After washing twice in PBS, the expression of CD80 on the surface of BMDCs was measured using the Gallios Flow Cytometer (Beckman Coulter, Brea, CA, USA), according to the manufacturer's instructions.

Antigen presentation assay.

The BMDCs were seeded in a 96-well culture plate at a density of 5×10^4 cells/well. After incubation at 37 ℃ for 24 h, sEVs were added to each well and then 1.5×10^5 BUSA14 cells or CD8-OVA1.3 cells were added. BUSA14 cells co-cultured with BMDCs treated with mouse $gp100_{25–33}$ (EGSRNQDWL; Anaspec Inc., Fremont, CA, U.S.A.) and Opti-MEM were used as positive and negative controls, respectively. CD8-OVA1.3 cells co-cultured with BMDCs treated with $OVA_{257-264}$ (SIINFEKL, InvivoGen, San Diego, CA) and Opti-MEM were used as positive and negative controls, respectively. After incubation for 24 h, the culture medium was centrifuged at 300 *g* for 3 min to collect the supernatants. The concentration of IL-2 in the supernatant was measured using mouse IL-2 enzyme-linked immunosorbent assay (ELISA) OptEIATM sets (Pharmingen, San Diego, CA, USA), according to the manufacturer's instructions.

Statistical analysis.

Statistical differences were evaluated using the Student's t-test for a paired-comparison and one-way analysis of variance (ANOVA) followed by the Tukey−Kramer multiple comparison test for multiple comparison. $P < 0.05$ was considered to be statistically significant.

I-3 Results

I-3-a CD40L-sEVs were successfully collected from B16BL6 cells transfected with pCMV-CD40L-LA plasmid DNA.

sEVs were harvested from B16BL6 cells that had been transfected with a plasmid DNA encoding fusion protein consisting of CD40L, LA, and FLAG (Figure 1A). The FLAG tag was fused with the CD40L-LA fusion protein for detection. The western blot analysis confirmed that sEV markers (Alix, HSP70 and CD81) were contained in the collected sEVs samples. As CD81, a member of transmembrane proteins, was not recovered in the cell lysate samples prepared by freezing-and-thawing cycles followed by centrifugation, CD81 was not detected in the cell lysates. The endoplasmic reticulum marker, calnexin, was not observed in the sEVs samples, indicating that the sEVs samples were not contaminated with cell debris. Furthermore, gp100, the melanoma antigen, was detected in the B16BL6 cells derived sEVs. Moreover, the FLAG tag was detected in CD40L-sEVs by Western blot analysis (Figure 1B), indicating successful modification of sEVs by CD40L.

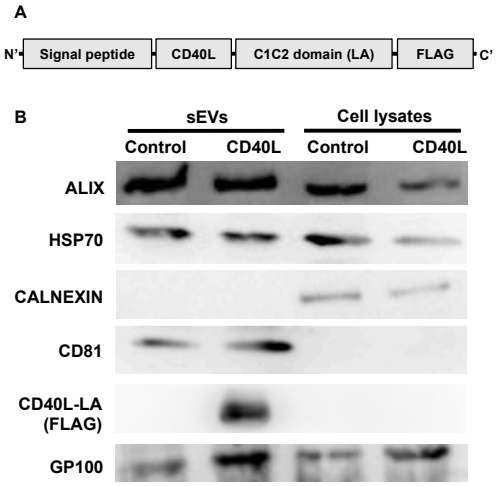

Figure 1. Design of plasmid DNA encoding CD40L-LA and identification of CD40L modification on sEVs. (A) A fusion protein consisting of CD40L, LA and FLAG was designed. (B) Western blot analysis of Alix, HSP70, Calnexin, CD81, FLAG (CD40L-LA) and GP100 in sEVs and cell lysates of unmodified sEVs (control) and CD40L-LA (CD40L) transfected B16BL6 cells.

I-3-b CD40L modification hardly changed the physicochemical properties of sEVs.

The particle size and morphology were assessed using the transmission electron microscope (TEM). The results (Figure 2A-B) revealed that the size and morphology of unmodified sEVs and CD40L-sEVs were almost identical. The zeta potential of sEVs was approximately -33mV, irrespective of CD40L modification (Figure 2C). Collectively, these findings demonstrate that modification by CD40L had little influence on the physicochemical properties of sEVs.

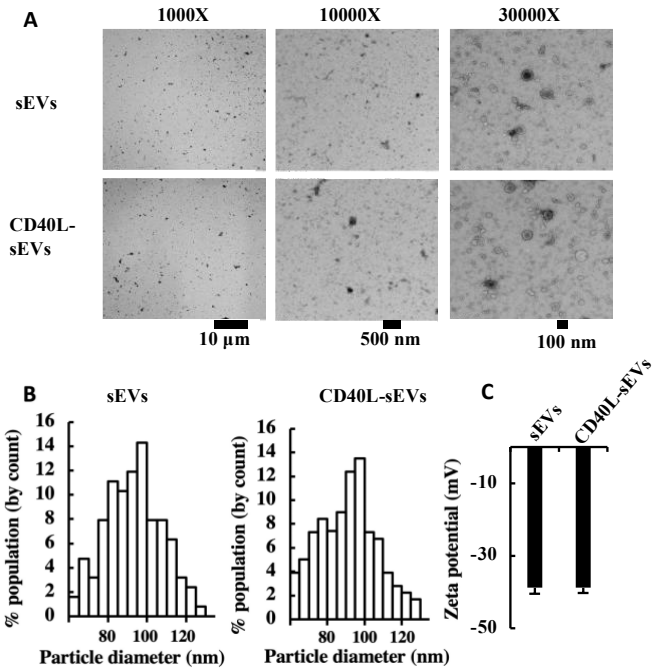

Figure 2. Characterization of CD40L-sEVs. (A) TEM images of sEVs and CD40L-sEVs. (B) Histograms of particle size distribution of sEVs and CD40L-sEVs obtained by analysis of TEM images. (C) Zeta potentials of sEVs and CD40L-sEVs. The results are expressed as means ± standard deviations (n=3).

I-3-c CD40L-sEVs were efficiently taken up by DC2.4 cells in a temperature-dependent manner.

To evaluate the effect of CD40L modification on the cellular uptake of sEVs by DCs, sEVs labeled with the green lipophilic fluorescent dye PKH67 were added to DC2.4 cells. The mean fluorescence intensity (MFI) values of DC2.4 cells treated with CD40L-sEVs were significantly higher than that of sEVs, indicating that CD40L modification enhanced cellular uptake of sEVs by DCs. Moreover, sEVs were hardly taken up by DC2.4 cells at 4°C (Figure

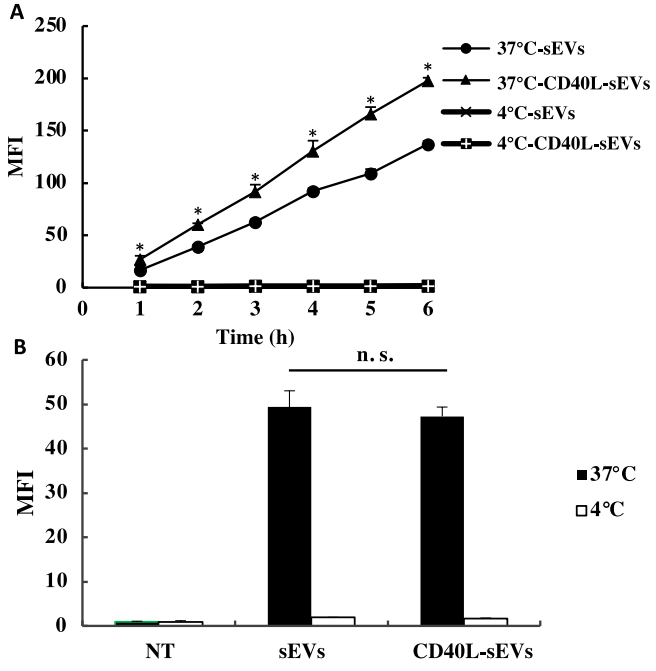

Figure 3. Uptake of CD40L-sEVs by DC2.4 cells and colon-26 cells. (A) Flow cytometric analysis of DC2.4 cells after the addition of PKH67-labeled sEVs and CD40L-sEVs at 37 ℃ and 4 ℃. (B) 4 h after the addition of PKH67-labeled sEVs and CD40L-sEVs, flow cytometric analysis of Colon-26 cells at 37 ℃ and 4 ℃. Results are expressed as the mean ± standard deviation (n = 4). *P < 0.05 compared with the other sEVs groups.

3A), which demonstrates that the internalization of sEVs by DCs is energy dependent. Additionally, colon-26 cells were selected as control cells because CD40, the receptor of CD40L is not expressed on the surface of colon-26 cells and colon-26 cells are non-immune cells. In the result of uptake experiment with colon-26, there was no significant difference in the MFI values of colon-26 cells treated with sEVs and CD40L-sEVs (Figure 3B), indicating that the modification of CD40L specifically enhanced the uptake of sEVs by DCs.

I-3-d CD40L-sEVs were mainly transported to the early endosome of DC2.4.

After internalization by the DC2.4 cells, the intracellular fate of sEVs was observed by confocal microscope. GFP loaded sEVs were added to the DC2.4 cells, early endosome marker (EEA1: early endosome antigen 1) and late endosome marker (LAMP1: lysosomal-associated membrane protein 1) were stained with Alexa Fluor647. Pearson's correlation (P) and Mander's overlap (M) of red and green signal were used as colocalization parameters. As P (0.20) and M (0.31) of CD40L-sEVs and EEA1 was higher than P (0.07) and M (0.20) of sEVs and EEA1, CD40L-sEVs were transported to the early endosome of DC2.4 cells more efficiently than sEVs (Figure 4A-B). On the other hand, as P (0.38) and M (0.42) of sEVs and LAMP1 was higher than P (0.08) and M (0.12) of CD40L-sEVs and LAMP1, unmodified sEVs were transported to the late endosome more efficiently than CD40L-sEVs (Figure 4A-B).

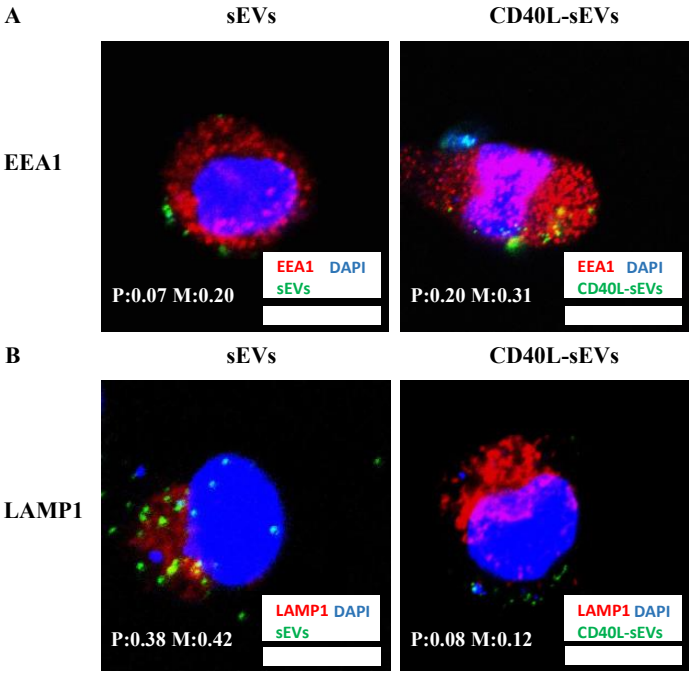

Figure 4. Intercellular fate of CD40L-sEVs after uptake of DC2.4. Confocal microscopy images of DC2.4 cells with sEVs and CD40L-sEVs. Green, GFP (sEVs). Blue, DAPI (nucleus). (A) Red, Goat Anti-Rabbit IgG H&L (Alexa Fluor® 647), (early endosome). (B) Red, Goat Anti-Rabbit IgG H&L (Alexa Fluor® 647), (late endosome). P: Pearson's correlation. M: Mander's overlap. Scale bar = 10 μm.

I-3-e BMDCs were efficiently activated by CD40L-sEVs.

To evaluate whether CD40L modification can activate the DCs, the BMDCs were incubated with sEVs and CD40L-sEVs. Significantly higher concentrations of IL-12p40 and TNF-α were observed in the CD40L-sEVs added group compared to the sEVs group (Figure 5A-B). Moreover, the number of BMDCs with high expression of the co-stimulatory molecule CD80 (B7), which can be regarded as highly activated BMDCs with fluorescence intensity of more than 10^2, was more in CD40L-sEVs group (~35 %) compared with sEV (~23%) (Figure 5C).

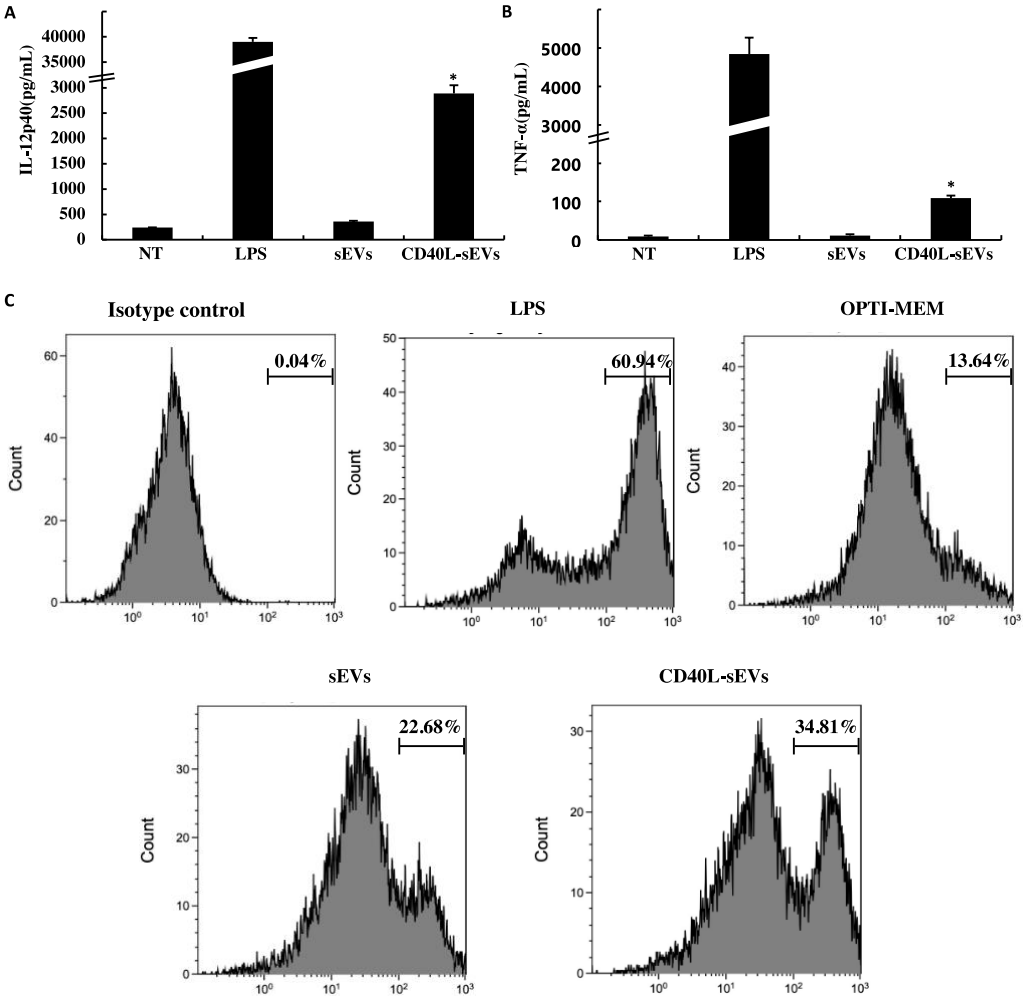

Figure 5. Activation of BMDCs by CD40L-sEVs. (A) IL-12p40 and (B) TNF-α secretion from BMDC cells after co-culture with Opti-MEM (NT), LPS, sEVs and CD40L-sEVs. *P < 0.05 compared with the sEVs group. The results are expressed as the mean ± standard deviation (n = 4). (C) Expression of CD80 on the surface of BMDCs after the addition of sEVs, analyzed by flow cytometry.

I-3-f BMDCs treated with CD40L-sEVs showed a higher MHC class I melanoma antigen presentation ability than those treated with unmodified sEVs.

BUSA14 cells, T-cell hybridoma cells capable of recognizing both human and mouse melanoma antigen gp100 presented on MHC class I molecules, were co-cultured with BMDCs treated with sEVs and CD40L-sEVs. The concentration of IL-2 released from BUSA14 cells in the culture medium was evaluated as the indicator of antigen presentation efficiency. CD40L modification enhanced the level of IL-2 secretion from BUSA14 cells co-cultured with BMDCs, indicating that the modification of CD40L significantly increased the ability of MHC class I melanoma antigen presentation of BMDCs treated with sEVs. On the other hand, in order to confirm the specificity of the response against melanoma antigen, I selected CD8-OVA1.3 cells, T-cell hybridoma cells capable of recognizing ovalbumin epitope presented on MHC class I molecules, as negative control T cells. B16BL6 cells derived sEVs and CD40L-sEVs were added to BMDCs and were co-cultured with CD8-OVA1.3 cells. There was no significant difference in IL-2 secretion from CD8-OVA1.3 cells between sEVs and CD40L-sEVs groups, indicating that CD40L-sEVs increased the ability of MHC class I melanoma-specific antigen presentation of BMDCs. (Figure 6)

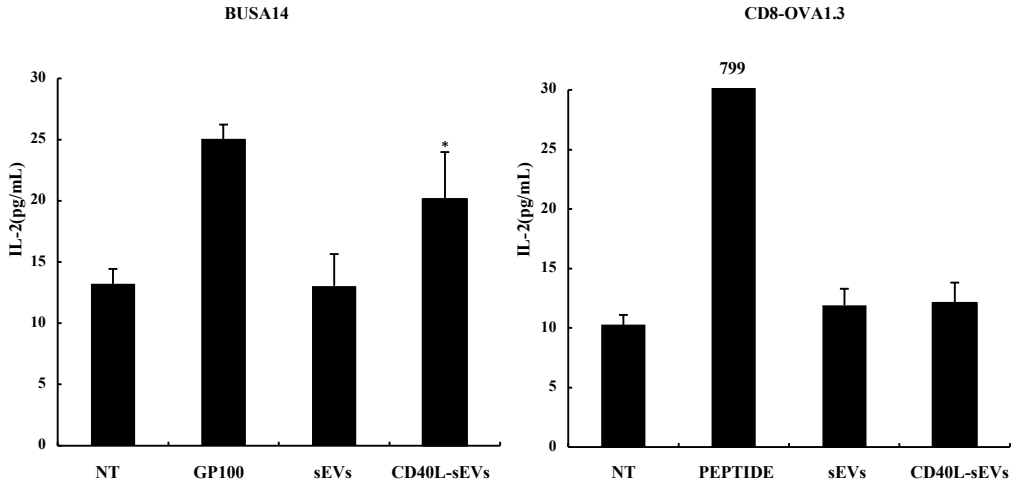

Figure. 6. Antigen presentation ability of BMDCs treated with sEVs. BMDCs were treated with Opti-MEM, peptides ($gp100_{25\text{-}33}$ for BUSA14 cells, $OVA_{257\text{-}264}$ for CD8-OVA1.3 cells), sEVs and CD40L-sEVs. Then, BUSA14 cells and CD8-OVA1.3 cells were added, and the cells were cultured for 24 h. The IL-2 concentration of the supernatants was measured. *$P < 0.05$ compared with sEVs group. The results are expressed as the mean ± standard deviation (n = 4).

I-4 Discussion

Targeting antigens to DCs by fusing ligands of protein expressed on the surface of DCs with antigens was regarded as an effective approach to obtain strong immune response[29]. Herein, CD40L, the ligand of CD40 on the surface of DCs, was fused with the C1C2 domain of the lactadherin protein and CD40L-modified endogenous tumor antigen containing multifunctional sEVs were collected. The LA protein was selected to serve as an anchoring scaffold because of its high efficiency in modification[30]. The CD40L-LA fusion protein was tethered to the surface of sEVs and can target CD40 on the surface of DCs with little changes in the physical properties of sEVs (Figure 2).

CD40L modification increased the uptake of sEVs by DCs. It is known that an CD40-bound antigen can be incorporated into recipient cells via endocytic pathway[31–33]. Almost all endocytic pathways are energy dependent processes, inhibited by low temperature[34]. Consequently, even though CD40L interacted with CD40 on the surface of DCs, the sEVs uptake level at 4°C was dramatically reduced, which confirmed the energy dependent uptake of CD40L-sEVs by DCs. On the other hand, if DCs internalized antigen by the CD40, the antigen is targeted towards a distinct pool of early endosomes[31]. It was reported that extracellular antigens targeted to early endosomes of DCs were processed and presented to T cells through the endosome-to-cytosol pathway[23,35]. In this study, I obtained the same results as those in the previous research described above, by confirming the co-localization of the green signal of GFP labeled CD40L-sEVs and the red signal of early endosome maker EEA1, while did not co-localize with the red signal of late endosome marker LAMP1 (Figure 4).

When CD40L-sEVs were incubated with DCs, the engagement of CD40 on the surface of DCs induced positive signaling that activated the NFκB pathway, resulting in the release of cytokines such as IL-12. As the production of IL-12 can increase Th1 differentiation of $CD4^+$ T cells[36] and the activated CD4+ T cells also possess CD40L[21], it is expected that activation of DCs by CD40L-sEVs can further activate the DCs to produce more immune activation cytokines such as IL-12 and IFN-γ to increase T cell-mediated immune responses[37].

In the antigen presentation assay, it was indicated that DCs treated with CD40L-sEVs showed an ability to present tumor antigen to $CD8^+$ T cells through MHC class I molecules (Figure 6). The reasons could be: (1) the enhanced presentation activity of DCs activated by CD40 signaling. Costimulatory molecules and MHC class I expression in DCs are upregulated by the interaction of CD40 and CD40L, which enhances the antigen presentation ability of DCs[38] (2) increased uptake of sEVs with CD40L modification by DCs through endocytosis

via CD40, a surface receptor on the DCs[31]. Moreover, it was reported that proteins taken up by CD40-mediated endocytosis were mainly found in early endosome, which did not undergo rapid fusion with lysosome, and which prevented antigens from lysosomal degradation[19]. Therefore, the retention of CD40L-sEVs taken up by DCs in early endosome might contribute to the enhanced MHC class I presentation of tumor antigens via cross-presentation pathway. On the other hand, as CD8-OVA1.3 cells, T-cell hybridoma cells capable of specifically recognizing OVA, did not release IL-2 when co-cultured with BMDCs treated with CD40L-sEV, CD40L-sEV is capable of specifically inducing melanoma derived antigen such as gp100.

To prepare an effective and safe vaccine, tumor antigen loading, antigen delivery system and adjuvant are considered as three necessary components of vaccine research[39]. In this study, sEVs were selected as tumor antigen carrier because they contain inherent endogenous tumor antigen so that usage of sEVs can exclude the cumbrous process of tumor antigen preparation[14–16]. Moreover, modification of CD40L has double function including improvement of delivery efficiency (Figure 3-4) to the DC and adjuvant function (Figure 5-6). Even though there are some further research such as the experiment to estimate whether the effect by CD40L modification on delivery efficiency and adjuvant activity is effective enough to induce strong anti-tumor immune response, should be done, it is no doubt that CD40L modification of sEVs will be helpful for the development of endogenous tumor antigen containing sEVs-based tumor vaccination.

I-5 Summary of chapter 1

Chapter 1 demonstrated that endogenous tumor antigen containing sEVs modified with CD40L were efficiently taken up by DCs and activated them. Moreover, CD40L modification increased the MHC class I presentation ability of tumor antigens by DCs treated with sEVs. This chapter indicates that CD40L modification of sEVs will contribute to further development of endogenous tumor antigen containing sEVs-based tumor vaccination.

Chapter 2

Evaluation of effects of exogenous antigen localization in antigen-loaded sEVs on efficiency of antigen presentation

II-1 Introduction

In chapter 1, I successfully developed CD40L-modified endogenous tumor antigen containing multifunctional sEVs with DC targeting, activation functions. To enable the development of new types of multifunctional sEVs, the incorporation of exogenous antigens into sEVs has become a critical factor of multifunctional sEVs design.

Antigen proteins can be loaded into either the outer surface or inner surface of sEVs. Considering that the intracellular location where antigen proteins are primed, affects the efficacy of MHC class I and II antigen presentation, the localization of the antigen proteins loaded into sEVs might also affect their behavior upon cellular uptake, and the efficacy of MHC class I and II antigen presentation. However, there is limited information regarding the effect of localization of antigen proteins loaded in sEVs on the efficacy of antigen presentation, as well as the intracellular behavior of the loaded proteins after cellular uptake of sEVs.

It is possible to load an antigen protein in or onto sEVs by designing a fusion protein composed of the antigen protein and an sEV-tropic protein. In previous study, lactadherin (LA) was used to load proteins to the outer surface of sEVs. LA is an sEV-tropic protein that binds to the phosphatidylserine present in the outer membrane of sEVs through C-terminal lectin-type domains (C1/C2domains) of LA[25]. In addition, I also used virus-derived group-specific antigen (GAG) to load proteins inside sEVs. GAG is an sEV-tropic protein that binds to thephosphatidylinositol-4,5-bisphosphate [$PI(4,5)P_2$] present in the inner membrane of sEVs[40]. Therefore, I can load antigens either to the inner surface or outer surface of sEVs by using these proteins.

In this chapter, I investigated the effects of localization of the proteins loaded in the sEVs on the efficacy of antigen presentation, as well as on the intracellular behavior of the loaded protein in antigen presenting cells (APCs). To evaluate the intracellular behavior of loaded proteins, green fluorescent protein (GFP) was loaded to the inner surface and outer surface of sEVs using GAG and LA, respectively. To investigate the effects of the localization of antigen proteins in sEVs on antigen presentation efficiency, ovalbumin (OVA), a model antigen protein, was loaded to the inner surface and outer surface of sEVs. An antigen presentation assay was performed using the two types of OVA-loaded sEVs.

II-2 Materials & Methods

Mice and cells.

Eight weeks old male C57BL/6 mice were purchased from Shimizu Laboratory Supplies

Co., Inc. (Shizuoka, Japan). Protocols for all animal experiments were approved by the Animal Experimentation Committee of the Graduate School of Pharmaceutical Sciences, Kyoto University. Human Embryonic Kidney cells 293 (HEK293) purchased from American Type Culture Collection (ATCC; CRL-1573) were cultured in 10 % fetal bovine serum (FBS)-containing Dulbecco's modified Eagle's medium (DMEM; Nissui Co., Ltd., Tokyo, Japan). Mouse dendritic DC2.4 cells and Mouse T-cell hybridoma CD8-OVA1.3 cells were obtained and cultured as described in Chapter 1.

Generation of bone marrow derived dendritic cells (BMDCs).

To determine the antigen presentation capacity of sEVs, I collected BMDCs as described in chapter 1.

Designing of fusion proteins and construction of plasmid DNA (pDNA).

LA and GAG coding sequences were obtained as described in previous reports[25,40]. The OVA-encoding sequence was synthesized along with the C1C2 domain sequences of mouse LA and GAG using PCR, to obtain OVA-LA and GAG-OVA, respectively. The enhanced green fluorescent protein (GFP)-encoding sequence was derived from the pEGFP-N1 vector (BD Biosciences Clontech, Palo Alto, CA, USA) along with the C1C2 domain of LA and GAG using PCR, to obtain GFP-LA and GAG-GFP fusion sequences, respectively. Information regarding the primers used to synthesize the fusion proteins used in this study is available upon request. The cDNAs of OVA-LA, GAG-OVA, GFP-LA, or GAG-GFP were inserted into the BamHI/XbaI site of the pcDNA 3.1 vector (Invitrogen, Carlsbad, CA, USA).

Preparation of sEVs.

GFP-outer and GFP-inner-loaded sEVs were isolated from HEK293 cells transfected with GFP-LA and GAG-GFP-pDNAs, respectively, using PEI Max (Polysciences, Inc., Warrington, PA, USA) as described previously[26]. OVA-outer and OVA-inner-loaded sEVs were isolated from HEK293 cells transfected with OVA-LA and GAG-OVA-expressing pDNAs, respectively, using PEI Max. sEVs were isolated from culture supernatants of non-transfected and transfected cells according to the method described in chapter 1. sEVs thus collected were resuspended in phosphate buffered saline (PBS). The amounts of sEVs collected were estimated by quantifying protein concentration using the Bradford assay.

Confocal microscopy.

DC2.4 cells were seeded onto glass coverslips at a density of 1.5 × 10^4 cells/well and incubated for 24 h. The culture medium was replaced with fresh medium containing 100 nM LysoTracker Red DND-99 (Molecular Probes, Eugene, OR, USA) and then GFP-loaded sEVs were added to it. Cells were washed using PBS for 30 min, 1 h, 2 h or 4 h after sEV-addition and fixed with 4 % paraformaldehyde for 20 min to stop the cellular uptake of sEVs. Then, 300 nM of 4′,6′-diamidino-2-phenylindole (DAPI) was added and cells were incubated for 5 min. After washing with PBS, the coverslips were mounted using SlowFade Gold (Thermo Fisher Scientific) to prevent fluorescent fading. The prepared samples were observed using a confocal microscope (A1R MP, Nikon Instech Co., Ltd., Tokyo, Japan).

Transmission electron microscopy (TEM).

The sEV samples were observed by TEM according to the method described in chapter 1.

Measuring of zeta potential of sEVs.

Zeta potential of sEVs was measured according to the method described in chapter 1 .

Fluorescent labeling of sEVs.

sEV samples were stained by PKH67 according to the method described in chapter 1.

Western blotting.

OVA, HSP70, CD81, Alix and Calnexin of sEV samples and HEK293 cells were detected according to the method described in previous chapter.

Flow cytometry analysis of sEV-uptake by cells.

BMDCs were seeded in a 96-well culture plate at a density of 5.0 × 10^4 cells/well for 24 h before the addition of sEVs. PKH67-labeled non-transfected (NT) sEVs, OVA-LA and GAG-OVA-loaded sEVs were added to the cells and BMDCs were incubated for 24 h. Then, BMDCs were washed with PBS three times and harvested in PBS. The cellular uptake of PKH-67-labeled sEVs was determined using the Gallios Flow Cytometer (Beckman Coulter, Brea, CA, USA), according to the manufacturer's instructions. Data were analyzed using the Kaluza software (Beckman Coulter).

Flow cytometry analysis of MHC class I-OVA complex on the surface of DC.

DC2.4 cells were seeded in a 24-well culture plate at a density of 2.0×10^5 cells/well for 24 h before the addition of sEVs. OVA-LA and GAG-OVA-loaded sEVs were added to the cells at a concentration of 10 μg/mL and DC2.4 cells were incubated for 24 h. Then, DC2.4 cells were washed with PBS three times and harvested in PBS. DC2.4 cells were stained with $OVA_{257-264}$ (SIINFEKL) peptide bound to H-2Kb Monoclonal Antibody, PE, (Thermo Fisher Scientific) in a final concentration of 30 μM at 37°C for 2 h. After washed with flow stain buffer, DC2.4 cells were measured using the Gallios Flow Cytometer, according to the manufacturer's instructions. Data were analyzed using the Kaluza software.

In vitro antigen presentation assay.

BMDCs were seeded in a 96-well culture plate at a density of 5.0×10^4 cells/well for 24 h before addition of sEVs. Indicated concentrations of HEK293-derived sEVs were added to BMDCs, which were then co-cultured with CD8-OVA1.3 cells (1.0×10^5 cells/well) for 24 h. CD8-OVA1.3 cells co-cultured with BMDCs treated with $OVA_{257-264}$, MHC class I-restricted peptide epitope of ovalbumin (OVA) were used as a positive control, and CD8-OVA1.3 cells cultured with BMDCs treated with SIINFEKL (InvivoGen, San Diego, CA, USA), and Opti-modified Eagle's Medium (Opti-MEM), were used as negative controls. The medium used for the co-culture was collected, and the concentration of IL-2 in the medium was measured using mouse IL-2 enzyme-linked immunosorbent assay (ELISA) OptEIA™ sets (Pharmingen, San Diego, CA, USA) according to the manufacturer's instructions.

Statistical analysis.

Differences among groups were evaluated using the Tukey-Kramer method, and $P < 0.05$ was considered statistically significant.

II-3 Results

II-3-a GFP was detected in the cytoplasm of DC2.4 cells after cellular uptake of GFP-inner-loaded sEVs, but not after that of GFP-outer-loaded sEVs.

GFP-outer-loaded (GFP_{OUT}) and GFP-inner-loaded (GFP_{IN}) sEVs were isolated from cells transfected with pDNA encoding GFP-LA or GAG-GFP, respectively. DC2.4 cells, to which GFP_{OUT} or GFP_{IN} sEVs were added, were observed using confocal microscopy to visualize the intracellular distribution of GFP (Figure 7). Confocal microscopy results showed that the green

signal derived from GFP was detected in DC2.4 cells to which GFP_{IN} sEVs were added. The green signal of GFP did not co-localize with the red signal of LysoTracker Red, which indicates that GFP was not present in the endosome and might exist in the cytoplasm. Moreover, the intensity of the green signal coming from GFP in the cells gradually increased with time. On the other hand, the green signal was barely detected in DC2.4 cells to which GFP_{OUT} sEVs were added.

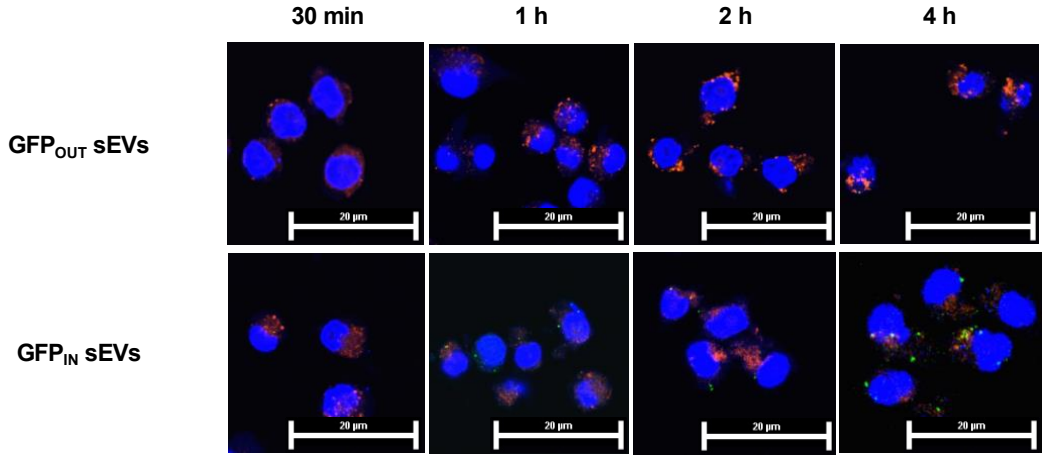

Figure 7. Confocal microscopy showing DC2.4 cells, to which GFP_{OUT} or GFP_{IN} sEVs were added. DC2.4 cells, to which GFP_{OUT} or GFP_{IN} sEVs and LysoTracker Red were added, were observed using confocal microscopy. Green, GFP. Blue, DAPI. Scale bar = 20 μm.

II-3-b Preparation of OVA-outer and OVA-inner-loaded sEVs.

pDNAs encoding OVA-LA and GAG-OVA were designed (Figure 8A). OVA-outer-loaded (OVA_{OUT}) and OVA-inner-loaded (OVA_{IN}) sEVs were isolated from cells transfected with the pDNA encoding OVA-LA or GAG-OVA, respectively. Western blotting analysis of the sEVs collected showed that OVA was loaded to the sEVs (Figure 8B). Moreover, to degrade proteins in outer surface of sEVs, OVA_{OUT} and OVA_{IN} sEVs were treated with Protease K and were subjected to western blotting analysis. OVA was detected in OVA_{IN} sEVs treated with protease K (Figure 8C) whereas, OVA was not detected in OVA_{OUT} sEVs after the treatment, which suggests that OVA loaded to the inner surface of sEVs was protected from degradation by the protease.

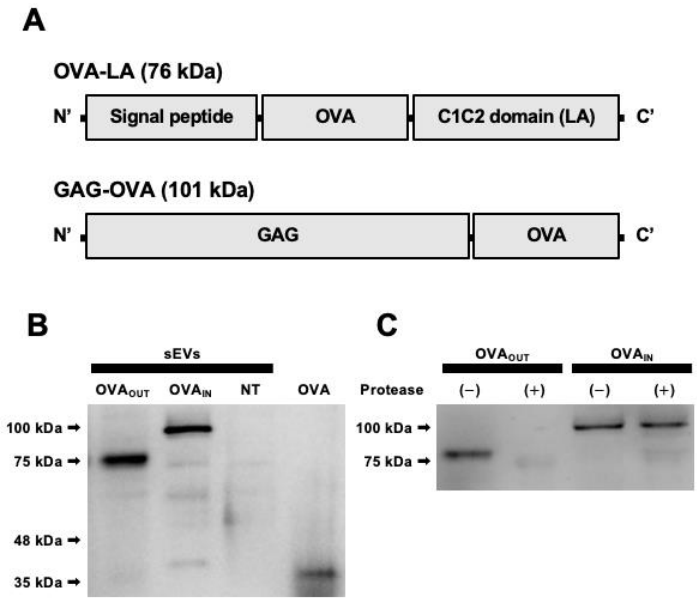

Figure 8. Design of pDNAs encoding OVA-LA or Gag-OVA, and detection of OVA loaded to sEVs. (A) Design of pDNAs encoding fusion proteins consisting of OVA-LA (76 kDa) or Gag-OVA (101 kDa). (B) Western blotting analysis of 5 μg of OVA_{OUT} and OVA_{IN} sEVs using anti-OVA antibody. Arrows indicate positions of the bands of molecular weight markers. (C) After treatment with or without protease, 5 μg of OVA_{OUT} and OVA_{IN} sEVs were analyzed using western blotting using the anti-OVA antibody. Arrows indicate positions of the bands of molecular weight markers.

II-3-c Properties of OVA_{OUT} and OVA_{IN} sEVs are almost identical to those of antigen-unloaded sEVs.

Western blotting for the three sEV marker proteins, HSP70, CD81, and Alix, was performed to verify the properties of OVA-loaded sEVs (Figure 9A). HSP70, CD81, and Alix were detected in all sEVs isolated from HEK293 cells. All sEVs showed negative results for Calnexin, an endoplasmic reticulum marker, which suggests little contamination from cell-derived debris in the sEV samples collected. Then, sEVs were observed using TEM (Figure 9B). TEM data revealed that the size of all sEVs was approximately 100 nm in diameter. Zeta potential values for sEVs OVA_{OUT} and OVA_{IN}, and sEVs collected from non-transfected cells (NT sEVs) were -39.2 ± 2.6, -37.3 ± 2.6 and -38.8 ± 1.3 (mV), respectively (Figure 9C). These results suggested that OVA loading scarcely altered the properties of sEVs.

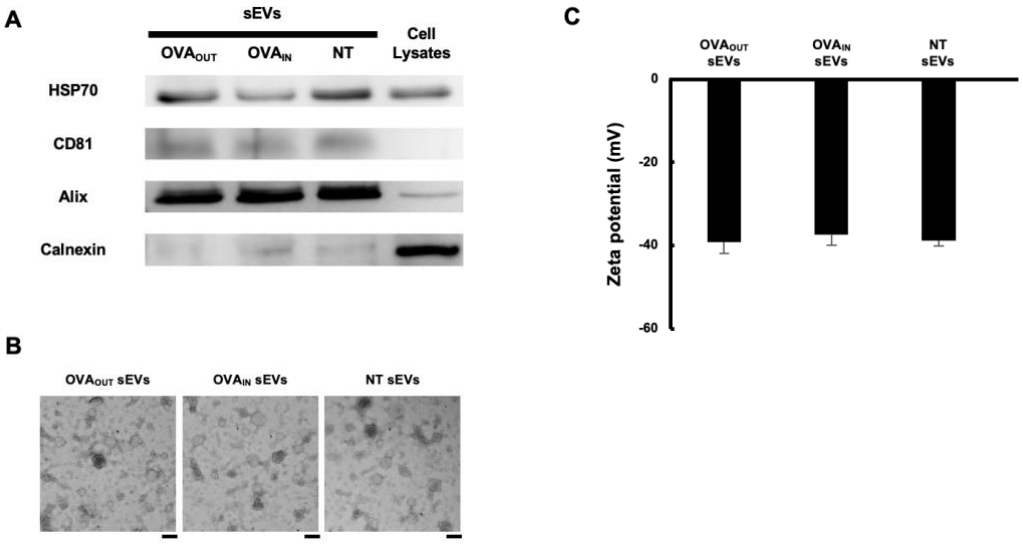

Figure 9. Properties of sEVs were scarcely affected by OVA-loading. (A) Western blotting for HSP70, CD81, Alix, and Calnexin in OVA_{OUT}, OVA_{IN} sEVs, NT sEVs and HEK293 cell lysates. (B) TEM images of OVA_{OUT}, OVA_{IN} sEVs and NT sEVs. Scale bar = 100 nm. (C) Zeta potential values for OVA_{OUT}, OVA_{IN} sEVs and NT sEVs. Results are expressed as the mean ± standard deviation (n = 4).

II-3-d Cellular uptake of sEVs by BMDCs was not affected by the localization of OVA in the sEVs.

To evaluate the uptake of OVA-loaded sEVs by BMDCs, NT sEVs and OVA-loaded sEVs fluorescently labeled with PKH67 were added to BMDCs, and the BMDCs were analyzed using flow cytometry (Figure 10). Flow cytometry results showed that there was no significant difference in mean fluorescent intensity (MFI) between BMDCs containing NT sEVs, OVA_{OUT} and OVA_{IN} sEVs, which suggests that localization of OVA in sEVs had little influence on cellular uptake of sEVs.

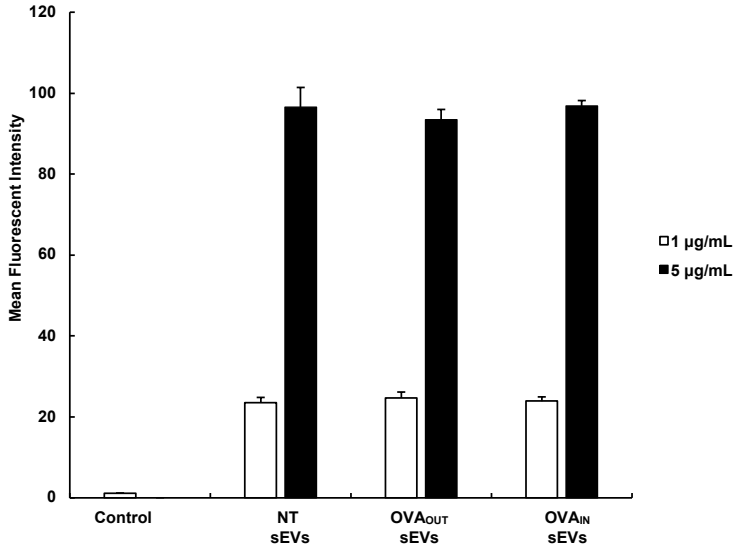

Figure 10. Cellular uptake of sEVs by BMDCs was almost identical between NT sEVs, OVA_{OUT} and OVA_{IN} sEVs. NT sEVs, OVA_{OUT} and OVA_{IN} sEVs were labeled using the PKH67 green fluorescent cell linker kit. C57BL/6 mice derived BMDCs were seeded at a density of 5.0×10^5 cells/mL. After 24 h of culture, 1 and 5 µg/mL of PKH-67-labelled NT sEVs, OVA_{OUT} or OVA_{IN} sEVs were added to each well 4 h before eliminating the supernatant. The uptake of sEVs by BMDCs was measured using fluorescence-activated cell sorting (FACS) analysis. Results are expressed as the mean ± standard deviation (n = 4).

II-3-e BMDCs containing OVA_{IN} sEVs cross-presented OVA-epitope to CD8-OVA1.3 cells through MHC class I.

To evaluate the efficiency of MHC class I antigen presentation, two experiments were performed. First, MHC class I-OVA complex displayed on the surface of DC was evaluated. DC treated with OVA_{IN} sEVs showed a higher expression of MHC class I-OVA complex than DC treated with OVA_{OUT} sEVs (Figure 11A). Second, NT sEVs, OVA and OVA_{OUT} or OVA_{IN} sEVs were added to BMDCs co-cultured with CD8-OVA1.3 cells. T cells secrete IL-2 upon cross-presentation of an antigen by DCs to CD8 positive T cells through MHC class I. ELISA analysis showed that the concentration of IL-2 secreted by CD8-OVA1.3 cells with OVA_{IN} sEVs was significantly higher as compared to that secreted by cells with NT sEVs and OVA_{OUT} sEVs in a concentration-dependent way (Figure 11B).

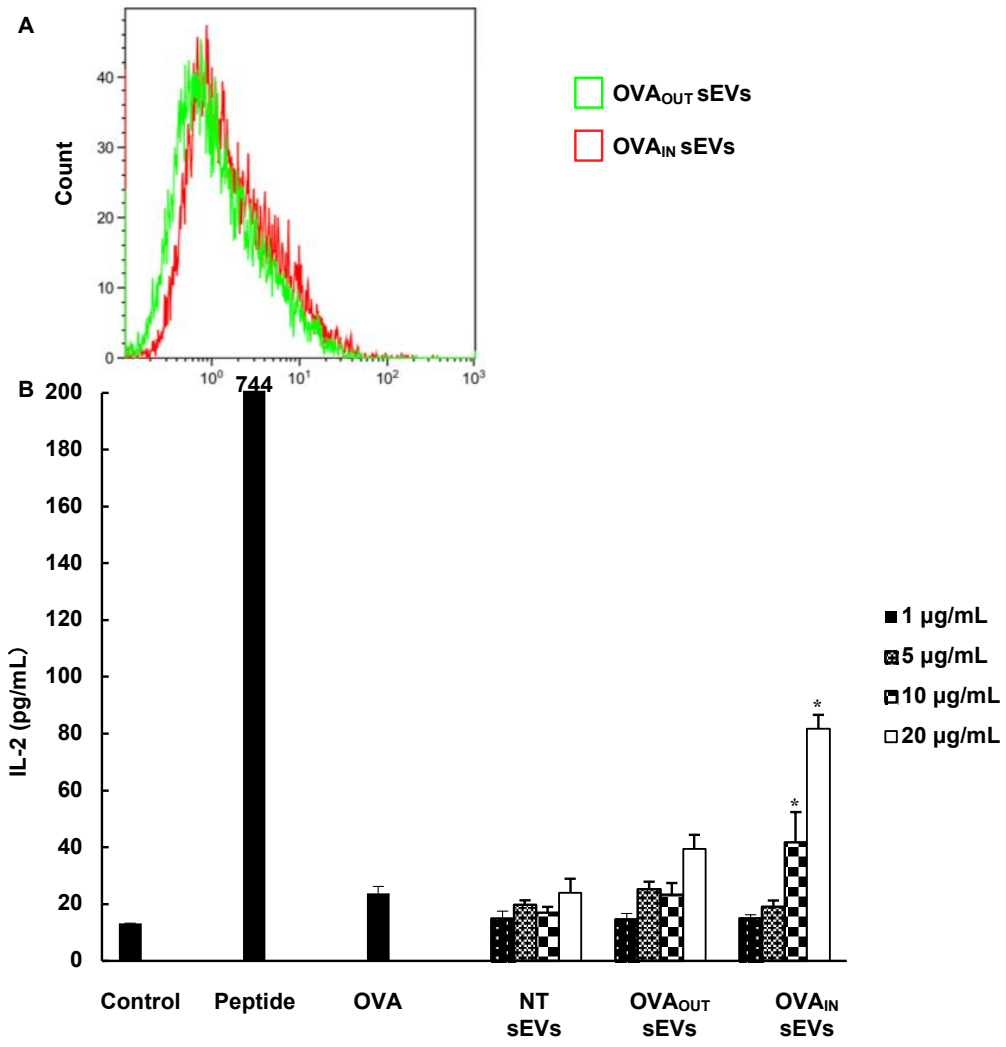

Figure 11. OVA epitope was presented by BMDCs added with OVA_{IN} sEVs but not OVA_{OUT} sEVs. (A) OVA_{OUT} and OVA_{IN} sEVs were added to the cells and DC2.4 cells were incubated for 24 h. The expression level of MHC class I-OVA complex was measured by FACS. (B) BMDCs derived from C57BL/6 mice were seeded (5.0×10^5 cells/ml). After 24 h of culture, OVA, NT sEVs, OVA_{OUT}, OVA_{IN} sEVs, or MHC class I specific peptide, and CD8-OVA1.3 (1.0×10^6 cells/ml) were added to the BDMC culture for a 24 h incubation. IL-2 concentration of the co-culture supernatants was measured using ELISA. *$P < 0.05$ compared with the other sEVs groups in the same concentration. Results are expressed as the mean ± standard deviation (n = 4).

II-4 Discussion

To elucidate the influence of the localization of antigen proteins in sEVs on their cytoplasmic distribution and antigen presentation, LA and GAG were selected to design fusion proteins according to the previous study[25,40]. Subsequently, I demonstrated that

proteins of interest, GFP and OVA, were loaded to the inner surface or outer surface of sEVs, respectively as seen in the physiological scenario. In the present study, MHC Class I presentation by DCs added with antigen-loaded sEVs was evaluated because induction of cellular immune response is more important than that of humoral immune response in cancer vaccination, which is one of the most expected application of sEVs-based vaccine. However, considering that more broad application of sEVs as vaccine, evaluation of MHC class II-mediated presentation should be considered in the further research.

sEVs may be taken up by clathrin-mediated or clathrin-independent endocytosis such as phagocytosis, micropinocytosis, and endocytosis via caveolae and lipid rafts[41]. After cellular uptake, sEVs are transported into lysosomes through the formation of multivesicular endosomes (MVEs) and are then degraded by low pH in the endosome and by proteases in the lysosome. Protease treatment of OVA_{OUT} sEVs degraded the loaded OVA protein, whereas the treatment hardly degraded OVA from OVA_{IN} sEVs, thus, proteins loaded outer surface of sEVs were more susceptible to intracellular degradation as compared to proteins loaded inside sEVs, results obtained using GFP-loaded sEVs suggest that GFP in GFP_{IN} sEVs was protected by the membranes of sEVs from degradation in the endosome/lysosome.

MHC class I presentation of OVA was higher in BMDCs with OVA_{IN} sEVs than that in BMDCs with OVA_{OUT} sEVs, whereas cellular uptake of OVA was comparable between these two groups. These results imply that antigen processing efficiency after cellular uptake of sEVs is different between DCs with OVA_{IN} sEVs and OVA_{OUT} sEVs. As OVA loaded in OVA_{IN} sEVs was protected by the membranes of sEVs from degradation after cellular uptake, OVA loaded in OVA_{IN} sEVs might be transferred to the cytoplasm more efficiently than that in OVA_{OUT} sEVs (Figure 7). A previous study reported that lymphoid organ resident $CD8^+$ DCs efficiently perform MHC class I antigen presentation by inhibiting degradation of antigens in endosomes/lysosomes by maintaining an alkaline pH in the endosome and phagosome[42]. Another study showed that efficient antigen presentation was promoted by loading antigen proteins onto cationic liposomes, which alkalinized the pH in the lysosomes of DCs[43]. The results obtained by the current study are in agreement with the results of previous studies and suggest that protection of antigen proteins from degradation in endosomes/lysosomes plays a significant role in increasing the efficacy of MHC class I antigen presentation.

II-5 Summary of chapter 2

Chapter 2 demonstrates that the localization of antigen proteins loaded in sEVs, inner surface or outer surface, alters their fate in cells. It was demonstrated that proteins loaded inside of sEVs were delivered to the cytoplasm of the cells that took up sEVs more efficiently than the proteins loaded outside of sEVs. Therefore, inner loading is effective for immunotherapy using exogenous antigen loading sEVs.

Chapter 3

Development of allergic rhinitis immunotherapy using exogenous allergen-loaded multifunctional sEVs

III-1 Introduction

In chapter 2, I optimized the method of loading exogenous antigen into sEVs and found that inner loading of exogenous antigen is more effective than outer loading. In this chapter, I explored the possibilities of exogenous antigen-loaded multifunctional sEVs in the treatment of immune diseases, especially allergic rhinitis.

Allergic rhinitis is triggered by breathing allergens such as dust mites and pollen. The patient's immune system overreacts to the allergens and exacerbates symptoms such as sneezing, nasal congestion, nasal itching, and rhinorrhea[44]. The number of patients with allergic rhinitis has been increasing worldwide in recent years and is associated with high socioeconomic costs[45]. For the treatment of allergic rhinitis, symptomatic treatment using antiallergic drugs that suppress the action of the immune system is currently in the mainstream, and it is desirable to develop a treatment method that enables radical treatment[46].

Allergen-specific immunotherapy (AIT) has been proven to be a radical treatment for allergic rhinitis[47]. However, AIT requires a long treatment time with multiple administrations, resulting in low patient adherence and therapy discontinuation[48]. Therefore, AIT should be optimized to achieve a relatively short and considerably efficient therapeutic effect. Various methods have been employed to boost the efficacy of AIT, including the development of new routes of administration, using allergen-derived peptides, or combining AIT with other interventions, such as adjuvants[46]. As an AIT adjuvant, CpG DNA can induce a T helper type 1 (Th1) immune response rather than T helper type 2 (Th2) immune response through recognition by Toll-like receptor 9 (TLR9)[49–51]. In previous preclinical studies and clinical trials, CpG DNA was tested as an AIT adjuvant with excellent outcomes[52,53]. Conversely, the co-delivery of CpG DNA and allergens is a challenge in the AIT research.

sEVs, which are cell-derived membrane vesicles with a diameter of approximately 100 nm, function as intercellular transport carriers that encapsulate proteins and nucleic acids[54]. sEVs are endogenous carriers, indicating that they are safer than other synthetic particles. Therefore, sEVs are powerful drug delivery systems[55]. In chapter 2, I found that ovalbumin (OVA), when loaded onto the inner surface of sEVs, can induce more efficient antigen presentation than when loaded onto the outer surface of sEVs[56]. Furthermore, previous findings have shown that CpG DNA can be added on the surface of sEVs as an adjuvant, modifying the sEVs[26]. Therefore, sEVs can be employed as co-delivery carriers for allergens and adjuvants.

In this chapter, OVA is selected as a model allergen and loaded onto the inner surface of sEVs using an sEV inner surface-tropic protein group-specific antigen (GAG)[40]. CpG DNA

is modified on the surface of the sEVs using an sEV surface-tropic protein, lactadherin (LA)[25]. The physicochemical properties of the CpG DNA-modified OVA-loaded sEVs (CpG-OVA-sEVs) are evaluated, and the uptake of CpG-OVA-sEVs by dendritic cells following the activation of the cells is evaluated *in vitro*. Afterward, I analyze the localization of the CpG-OVA-sEVs after intranasal administration in the nasopharynx-associated lymphoid tissue (NALT) in mice. Finally, using a mouse model of allergic rhinitis, the therapeutic effect of the CpG-OVA-sEVs on alleviated allergic symptoms and the immune system, including Th1/2 balance and IgE secretion, is evaluated.

III-2 Materials & Methods

Mice and cells.

Six-week-old male BALB/c mice were purchased from Japan SLC, Inc. (Shizuoka, Japan). Protocols for all animal experiments were approved by the Animal Experimentation Committee of the Graduate School of Pharmaceutical Sciences, Kyoto University. HEK293 and DC2.4 cells were obtained and cultured as described in previous chapters.

Oligodeoxynucleotides (ODNs).

All ODNs used in this study were purchased from Integrated DNA Technologies, Inc. (Coralville, IA, USA). Fully phosphorothioate-modified ODN containing a CpG motif (ODN 1668: 5'-TCCATGACGTTCCTGATGCT-3') was labeled with triethylene glycol (TEG)-biotin at the 3' end. CpG DNA labeled with 6-carboxy-fluorescein (FAM) at the 5' end and TEG-biotin at the 3' end was used to evaluate the modification efficiency as well as cellular uptake.

Preparation of the CpG-OVA-sEV and the fluorescent labeling of sEV.

Plasmid DNA encoding GAG-OVA and Streptavidin-LA (SAV-LA) were obtained as previously described[40,57]. HEK293 cells were simultaneously transfected with pCMV-GAG-OVA and pCMV-SAV-LA plasmid vectors using PEI MAX (Polysciences, Inc., Warrington, PA, USA) as described previously[26]. sEVs were collected from the culture supernatant as described in previous chapters. SAV-LA-sEVs were collected from the HEK293 cells transfected with the pCMV-SAV-LA plasmid vector, GAG-OVA-sEVs were collected from the HEK293 cells transfected with the pCMV-GAG-OVA plasmid vector, and SAV-LA-GAG-OVA-sEVs were collected from the HEK293 cells transfected with both the pCMV-GAG-OVA and pCMV-SAV-LA plasmid vectors. The amount of sEVs was estimated by

measuring the protein concentration using the Bradford assay. Subsequently, the SAV-LA-GAG-OVA-sEV (1 μg of protein) was incubated with 100 pmol biotinylated CpG DNA for 10 min at room temperature, washed with PBS, and ultracentrifuged for 2 h at 100,000 g to remove free CpG DNA. FAM-CpG-OVA-sEVs were obtained after the SAV-LA-GAG-OVA-sEVs reacted with the FAM-labeled biotinylated CpG DNA, as described above. After they were washed using PBS and ultracentrifuged, the sEV membranes were stained using a PKH26 red or PKH67 green fluorescent cell linker kit purchased from Sigma-Aldrich (St. Louis, MO, USA) for 5 min at room temperature. After stopping the reaction with PBS containing 5% bovine serum albumin (BSA) for 1 min at 25 °C, the fluorescently labeled sEVs were ultracentrifuged at 100,000 g for 2 h, washed, and resuspended in PBS.

Western blot.

ALIX, HSP70, CD81, Calnexin, SAV (1:100 dilution; antibody purchased from Sigma-Aldrich, USA)), and OVA of sEV samples and HEK293 cells were detected according to the method described in previous chapter.

Characterization of the physicochemical properties of CpG-OVA-sEV.

The sEV samples were observed by TEM according to the method described in chapter 1. The zeta potential of the sEVs was measured using a Zetasizer Nano ZS (Malvern Instruments, Malvern, UK).

Cellular uptake of sEVs by cells.

DC2.4 cells seeded in 96-well-plates at a density of 5.0×10^4 cells/well were cultured for 24 h at 37 °C. Subsequently, PKH67-labeled sEVs or FAM-CpG-OVA-SEVs suspended in Opti-MEM were added to the cells and incubated for 24 h at 37 °C. Afterward, the cells were washed three times in PBS and suspended in PBS. The cellular uptake of the sEVs was evaluated using a Gallios flow cytometer (Beckman Coulter, Brea, CA, USA) according to the manufacturer's instructions. Data were analyzed using the Kaluza software (Beckman Coulter). The mean fluorescent intensity (MFI) was calculated as an indicator of cellular uptake.

Cytokine release from DC2.4

DC2.4 cells were seeded in a 96-well culture plate at a density of 5×10^4 cells/well. After 24 h of incubation at 37 °C, the sEVs suspended in Opti-MEM were added to each well. The

DC2.4 cells treated with 10 ng/mL of lipopolysaccharide (LPS, Sigma-Aldrich St. Louis, MO, USA) and Opti-MEM were used as positive and negative controls, respectively. After the incubation at 37 °C for 24 h, the concentrations of the tumor necrosis factor (TNF)-α and IL-6 in the supernatant were evaluated according to the method described in chapter 1.

Preparation of frozen tissue sections and immunofluorescence

One day after the intranasal administration of FAM-CpG DNA or FAM-CpG-OVA-sEVs, the mice were sacrificed. The fur and skin of the skull were gently removed, and the cranium of the mouse was fixed in a 4% paraformaldehyde phosphate buffer solution (Nacalai Tesque, Kyoto, Japan) for 48 h at 4 °C. After rinsing with running tap water for 1 h, the sample was decalcified for 1 week at 4 °C, using decalcifying solution B (Wako FUJIFILM, Osaka, Japan). Subsequently, the sample was rinsed for 2 h using running tap water and immersed in 10% sucrose for 12 h, 15% sucrose for 12 h, and 20% sucrose for 12 h. After cleaning with filter paper, the sample was embedded with a Tissue-Tek O.C.T. compound (Sakura Finetek, CA, USA) and sectioned at a thickness of 8 μm. Half of the sections were observed using a fluorescence microscope (Biozero BZ-X710, Keyence, Osaka, Japan). The other half of the sections were fixed with a 4% paraformaldehyde phosphate buffer solution (Nacalai Tesque, Kyoto, Japan) for 20 min. After washing with PBS, the sections were stained with the following antibodies: BV421 hamster anti-mouse CD11c (BD Horizon, USA), Purified anti-mouse B220 (Biolegend, USA), and goat anti-rat IgG H&L (Alexa fluor@594) (Abcam, UK). The specimens were washed three times using PBS, embedded in Fluoro-KEEPER antifade reagent (Nacalai Tesque, Kyoto, Japan), and observed using a confocal microscope (A1R MP, Nikon Instech Co., Ltd., Tokyo, Japan).

Establishment of allergic rhinitis mice model and the estimation of the therapeutic effect of CpG-OVA-sEVs

The mouse models of allergic rhinitis were established based on a previously published method with minor modifications[58]. Briefly, six-week-old male Balb/c mice were intraperitoneally administered 0.25 mg/mL of OVA (Sigma-Aldrich St. Louis, MO, USA) and 10 mg/mL of aluminum hydroxide (Thermo Scientific, Waltham, MA, USA) in PBS at a dosage of 200 μL. The immunization was repeated three times (days 0, 7, and 14). After the daily intranasal administration of OVA (1 mg, 10 μL) from day 21 to day 27, blood samples were collected from each mouse. Serum IgE concentration was evaluated using the mouse IgE

ELISA OptEIA™ sets (Pharmingen, San Diego, CA, USA) according to the manufacturer's instructions. Afterward, the allergic rhinitis mice models were intranasally treated daily using PBS, GAG-OVA-sEV, CpG-sEV, and CpG-OVA-sEV (10 μg/dose). Re-challenge was followed by the consecutive and intranasal administration of OVA (1 mg, 10 μL) from day 35 to day 41. On day 40, following intranasal OVA administration, the number of nasal rubbing and sneezing was counted for 5 min. On day 42, the mice were sacrificed. The mouse skull, serum, and spleen were collected for subsequent estimation.

Evaluation of antigen specific Th1/Th2 immunity.

To evaluate the cytokines released from the splenocytes, splenocytes were seeded in a 48-well culture plate at a density of 5×10^6 cells/mL. After 3 days of co-culture using OVA or BSA, the concentration of IFN-γ in the supernatant was evaluated using a mouse IFN-γ ELISA kit (Thermo Fisher, Waltham, MA, USA) according to the manufacturer's instructions. For the measurement and isotyping of antibody production, a 0.1-M carbonate buffer containing OVA or BSA was applied to 96-well ELISA plates to coat each well. After incubating overnight at 4 °C, the plate was washed three times and blocked with 5% BSA for 1 h at room temperature. Subsequently, the plates were washed three times, and 100 μL aliquots of serial serum samples were added to each well. After 2 h of incubation, the plates were washed five times, and 100 μL of HRP-conjugated anti-mouse IgG1 and anti-mouse IgG2a antibody (1:3000; Bethyl Laboratories, Montgomery, TX, USA) were added to each well. After 1 h of incubation, each well was washed five times, and 200 μL of newly prepared O-phenylenediamine dihydrochloride (Wako FUJIFILM, Osaka, Japan) solution containing 0.04% hydrogen peroxide in phosphate-citrate buffer (Nacalai Tesque, Kyoto, Japan) was added to each well. After a 10 min incubation period, 50 μL of 10% H_2SO_4 was added to each well, and the absorbance was recorded at 450 nm.

Histological observation.

The fur and skin of the skull were gently removed, and the cranium of the mouse was fixed in 10% formaldehyde neutral buffer solution (Nacalai Tesque, Kyoto, Japan) for 48 h at room temperature. After rinsing with running tap water for 1 h, the sample was decalcified for 1 week at 4 °C using decalcifying solution B (Wako FUJIFILM, Osaka, Japan). Subsequently, the sample was rinsed with running tap water for 2 h and dehydrated using 70% alcohol for 30 min, 80% alcohol for 1 h, and 90% alcohol for 1 h, followed by three changes in duration for 100%

alcohol, 2 h, 2 h, 7.5 h. After dehydration, the samples were cleared using xylene at three duration: 30 min, 30 min, and 45 min. After that, the sample was immersed in paraffin for 30 min, 30 min, and 45 min. Finally, the sample was embedded in a paraffin block, and the paraffin-embedded sample block was sectioned with a thickness of 8 μm. The sections were stained using hematoxylin and eosin and observed under a microscope (Biozero BZ-X710, Keyence, Osaka, Japan).

Statistical analysis.

Statistical differences were evaluated using the student's t-test for a paired comparison and one-way analysis of variance (ANOVA) followed by the Tukey−Kramer multiple comparison test for multiple comparisons. $p < 0.05$ was statistically significant.

III-3 Results

III-3-a Preparation of CpG-OVA-sEVs

The plasmid DNA encoding fusion proteins of SAV-LA and GAG-OVA were simultaneously transfected to the HEK293 cells (Figure 12A). sEVs were collected from the transfected HEK293 cells by ultracentrifugation, and sEV markers (ALIX, HSP70, and CD81) were confirmed by western blotting. Calnexin, an endoplasmic reticulum marker, was not detected in the sEV samples, indicating that the sEV samples were not contaminated with cell

debris (Figure 12B). Moreover, the OVA band of the sEVs collected from the GAG-OVA-transfected cells was not eliminated by protease treatment, indicating that the GAG-OVA was loaded into the inner space of the sEVs. However, the SAV band of the sEVs collected from the SAV-LA-transfected cells was eliminated by protease treatment, indicating that the SAV-LA

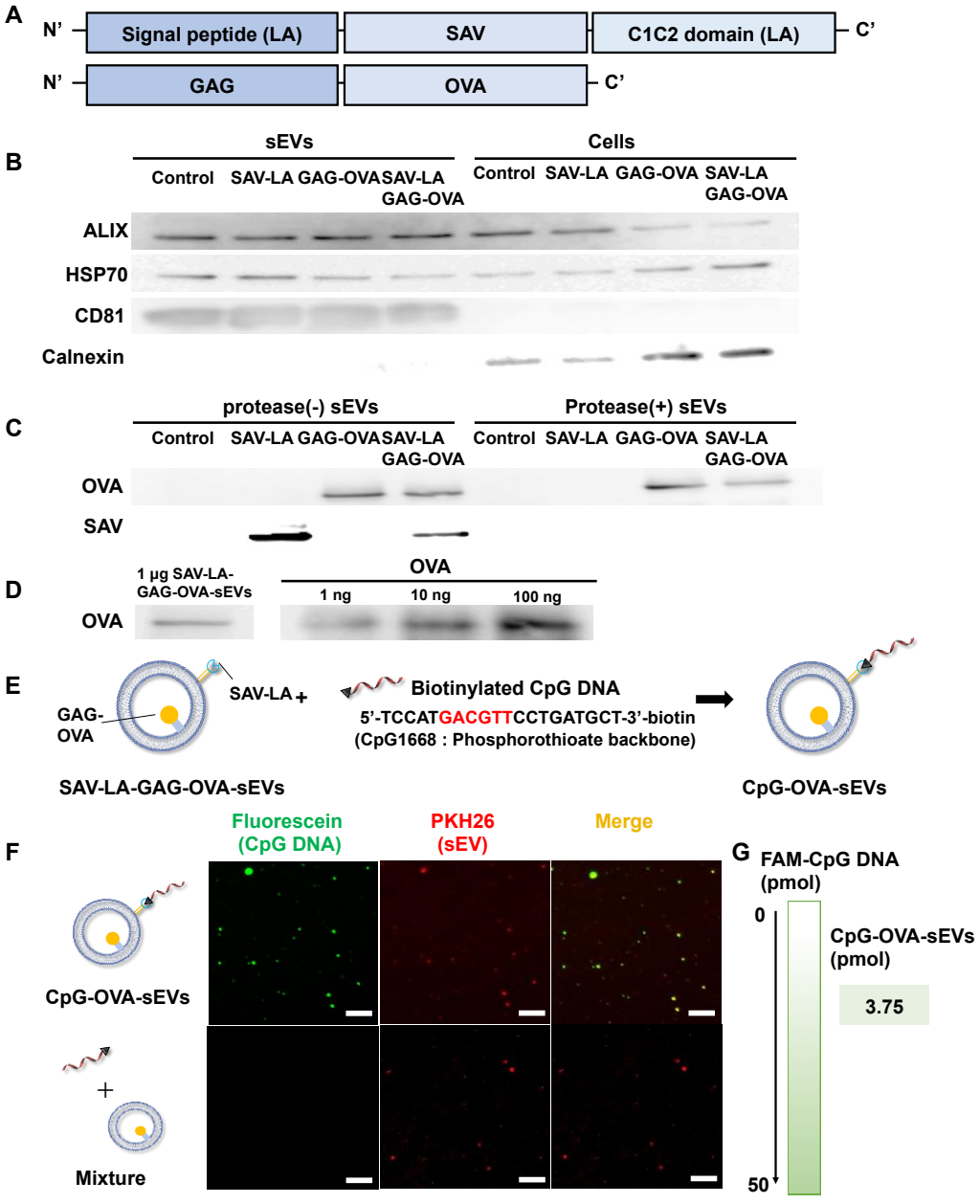

Figure 12. Preparation of CpG-OVA-sEVs. (A) Fusion proteins of GAG-OVA and SAV-LA were designed. (B–D) Western blot analysis of sEV markers (ALIX, HSP70, CD81), sEV negative marker (Calnexin), SAV, and OVA. (E) Illustration of CpG-OVA-sEV preparation. (F) Fluorescent microscopic observation of CpG-OVA-sEV, CpG DNA mixed with GAG-OVA-sEV. Scale bar = 50 μm. (G) Fluorescent intensity of the FAM-CpG DNA standard and the CpG-OVA-sEV.

was bound to the outer surface of the sEVs (Figure 12C). One microgram of SAV-LA and GAG-OVA showed that the sEVs (SAV-LA-GAG-OVA sEVs) contained approximately 1 ng of OVA (Figure 12D). Subsequently, the SAV-LA-GAG-OVA sEVs were interacted with biotinylated CpG DNA to harvest CpG-OVA-sEVs (Figure 12E). To confirm the CpG DNA modification, green FAM was labeled at the 5' end of CpG DNA, and SAV-LA-GAG-OVA sEVs were stained with red dye PKH26. After interacting with the FAM-labeled CpG DNA, CpG-OVA-sEVs showed co-localization of red and green signals (Figure 12F). Additionally, the FAM-labeled CpG DNA did not show any co-localization with the PKH26-labeled GAG-OVA-sEV, indicating that CpG DNA was modified to sEVs via an SAV–biotin interaction, and there was no free CpG DNA after PBS washing by ultracentrifugation (Figure 12F). One microgram of CpG-OVA-sEV contained approximately 3.75 pmol of CpG DNA, corresponding to 1076 CpG DNA molecules per sEV (Figure 12G).

III-3-b The physicochemical properties of sEV were not altered by the modification of GAG-OVA and CpG DNA.

The particle size and morphology of the sEVs were observed using a TEM. The results (Figures 13A–C) revealed that there was no agglomeration in each sEV group and that there was little difference in the size and morphology among all the sEV groups. The zeta potential of each sEV group was approximately −32 mV, regardless of the GAG-OVA and CpG DNA modification (Figure 13D). These results showed that the modification of GAG-OVA and CpG DNA had little influence on the physicochemical properties of the sEVs.

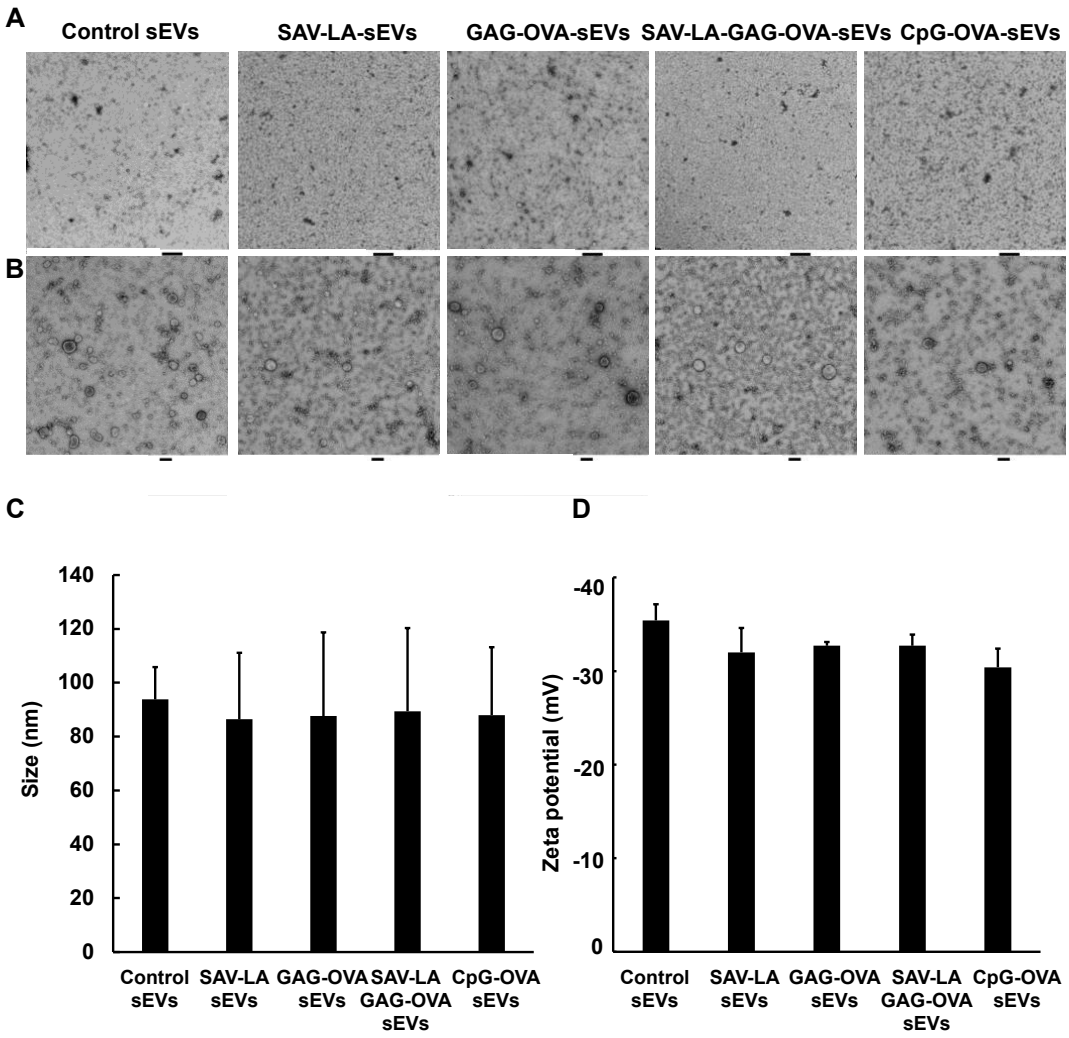

Figure 13. Characterization of the physicochemical properties of CpG-OVA-sEVs. (A) TEM images (X10000) of the control sEVs, SAV-LA-sEVs, GAG-OVA-sEVs, SAV-LA-GAG-OVA-sEVs, and CpG-OVA-sEVs. Scale bar = 500 nm. (B) TEM images (X30000) of the control sEVs, SAV-LA-sEVs, GAG-OVA-sEVs, SAV-LA-GAG-OVA-sEVs, and CpG-OVA-sEV. Scale bar = 100 nm. (C) Particle size and (D) zeta potential of the control sEVs, SAV-LA-sEVs, GAG-OVA-sEVs, SAV-LA-GAG-OVA-sEVs, and CpG-OVA-sEVs. The results are expressed as means ± standard deviation (n = 3).

III-3-c CpG DNA can be efficiently delivered to dendritic cells via an sEV and can activate dendritic cells *in vitro*.

To identify whether CpG DNA modification influences the uptake of the sEVs by dendritic cells, each sEV group was stained with the lipophilic carbocyanine green dye PKH67 and was subsequently co-cultured with DC2.4 cells. The MFI values of the DC2.4 cells treated with

each sEV group were not significantly different, indicating that the CpG DNA modification had no influence on the uptake of sEVs by dendritic cells (Figures 14A–B). However, when fluorescent dye FAM was labeled at the 5' end of the CpG DNA, the DC2.4 cells treated with FAM-CpG-OVA-sEVs showed a higher MFI value than other groups, suggesting that the uptake of the CpG DNA by dendritic cells was increased by modifying the CpG DNA on the sEVs (Figures 14C–D). Moreover, to examine the dendritic cell activation effect of the CpG-OVA-sEVs, the DC2.4 cells were incubated with each sEV group. Resultantly, remarkably higher concentrations of TNF-α and IL-6 were observed in the culture medium of the CpG-OVA-sEVs-treated DC2.4 cells than in the other groups, showing that the CpG-OVA-sEVs can activate dendritic cells *in vitro* (Figures 14E–F).

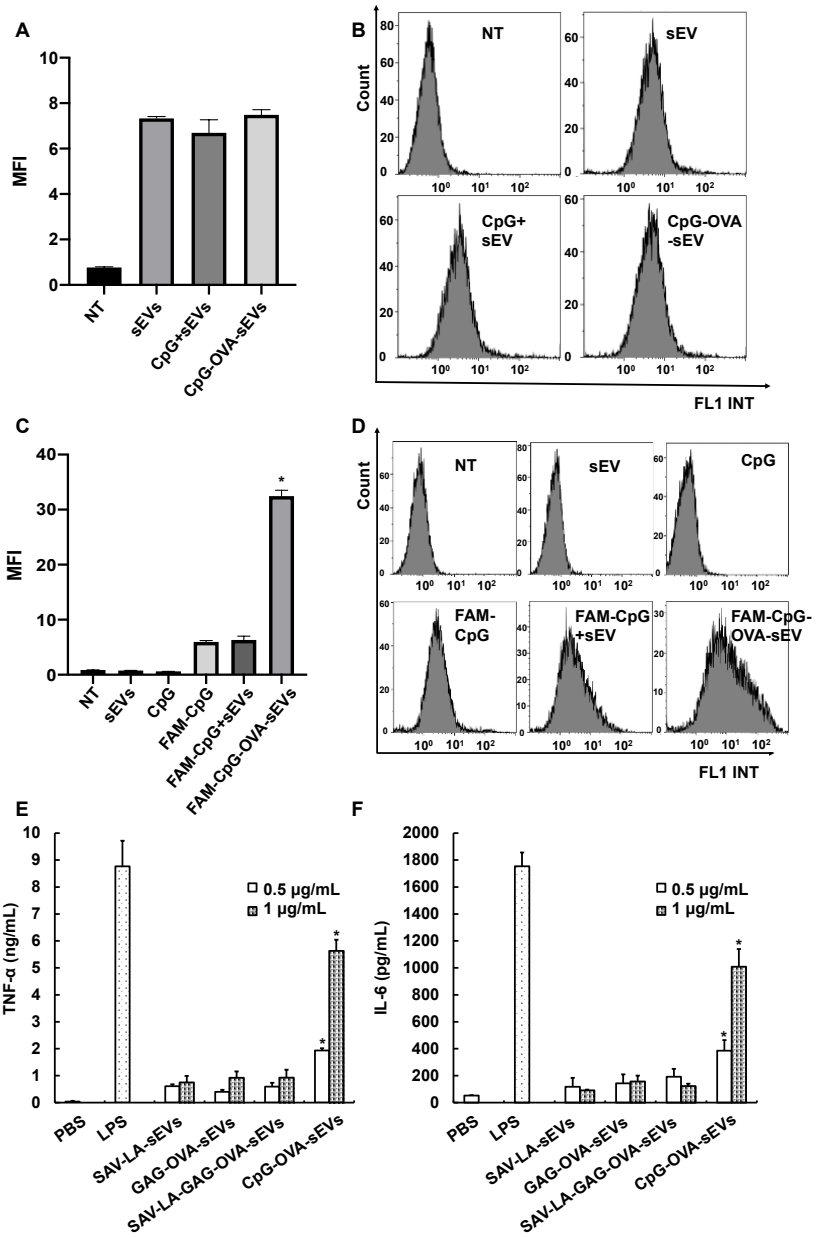

Figure 14. Uptake of CpG-OVA-sEV by dendritic cells and the activation of dendritic cells by CpG-OVA-sEV. (A–B) Flow cytometric analysis of the DC2.4 cells after co-culturing with PKH67-stained sEV. (C–D) Flow cytometric analysis of the DC2.4 cells after co-culture with FAM-labeled sEV. (E) TNF-α and (F) IL-6 concentration in the supernatant of the DC2.4 cells after co-culture with the sEV. *$p < 0.05$ compared with the other groups. The results are expressed as means ± standard deviation (n = 4).

III-3-d CpG-OVA-sEVs were delivered to the NALT of the mouse.

After the CpG-OVA-sEVs were intranasally administered to the mice, the skulls of the mice were recovered, and thereafter, the NALTs of the mice were collected using a cryostat. The NALT in mice is localized on the soft palate of the upper jaw and can be histologically identified as a triangular shape (Figure 15A). The green fluorescence of the FAM-labeled-CpG-OVA-sEVs was observed in the NALT of the CpG-OVA-sEV group, but not in the NT and FAM-labeled CpG DNA groups (Figures 15B–C). Subsequently, I stained the NALT with immunofluorescence and found CD11c positive cells and B220 positive cells inside the NALT, with the CpG-OVA-sEV signal overlapping with some of the CD11c positive cells but not with the B220 positive cells (Figures 15B–C). Therefore, it is considered that the CpG-OVA-sEVs were delivered to the NALT of the mice after intranasal administration and were taken up by the CD11c positive cells in the NALT.

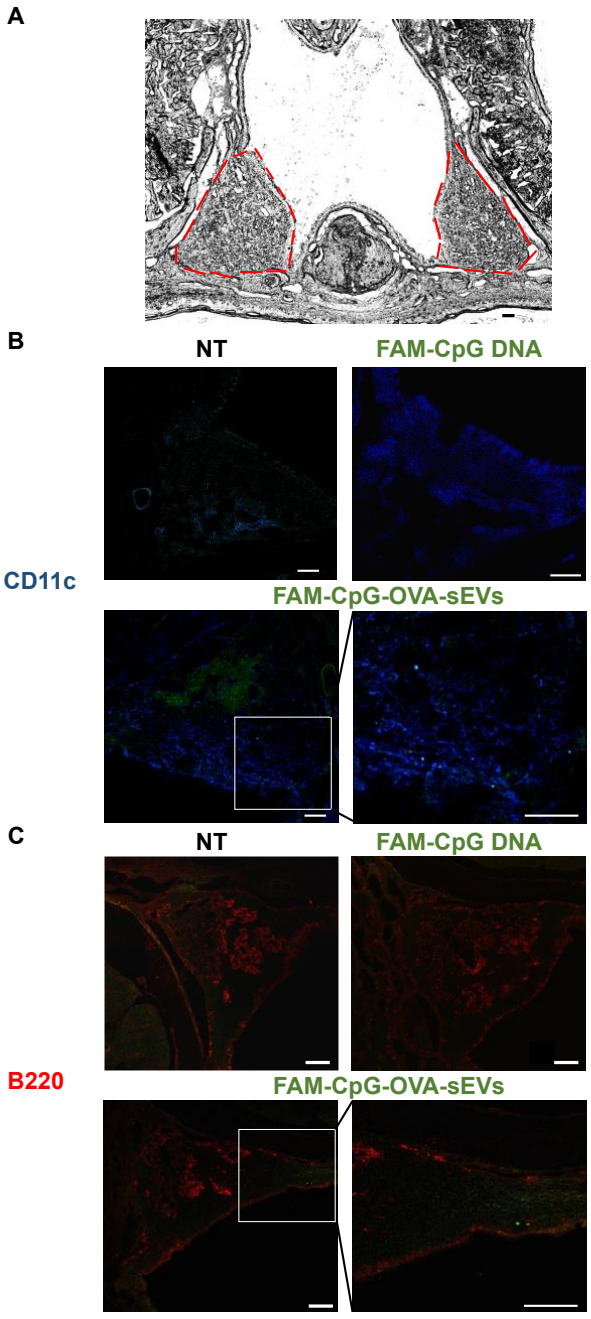

Figure 15. Observation of the frozen sections of the mouse. (A) Microscopic image of a frozen section of the NALT of a mouse. The NALT is circled in red. (B–C) Frozen sections of the NALT of the mouse were stained with the indicated fluorescent-labeled antibody after intranasally administrating FAM-CpG DNA, FAM-CpG-OVA-sEVs. Green = FAM-CpG DNA, or FAM-CpG-OVA-sEVs. Sections were observed by confocal microscopy. Scale bar = 50 μm.

III-3-e IgE secretion in mouse serum was reduced, and allergic symptoms were alleviated by CpG-OVA-sEVs administration compared with the control group.

To evaluate the therapeutic effect of CpG-OVA-sEVs, I prepared an allergic rhinitis mouse model according to the protocol shown in Figure 16A. After immunization and allergen challenge, IgE concentrations in the mouse serum were identical in each group (Figure 16B). However, upon treatment with CpG-OVA-sEVs and re-challenge with OVA, the IgE concentration in the serum was significantly reduced compared with the other groups (Figure 16C). Additionally, rubbing and sneezing numbers were counted after treatment with CpG-OVA-sEVs. Compared with the low numbers in NT mice, PBS and GAG-OVA-sEV mice showed higher rubbing and sneezing numbers, and in the CpG-OVA-sEV groups, the number of sneezing and rubbing was dramatically reduced (Figures 16D–E). To observe the nasal histological changes in each group, the mouse nasal sections were stained with hematoxylin and eosin. The section of the NT group showed normal nasal cavity mucosa with thin and flawless respiratory epithelium. The PBS group and GAG-OVA-sEV group revealed thick and damaged respiratory epithelium, mucosal exfoliation, and infiltration of numerous cells. Contrarily, in the CpG-OVA-sEV group, there was less infiltration of inflammatory cells, and the respiratory epithelium was thinner than in the PBS and GAG-OVA-sEV groups (Figures 16F–G). Conversely, the intranasal administration of the CpG-sEVs resulted in less therapeutic effects than that of the CpG-OVA-sEVs. In conclusion, CpG-OVA-sEV exhibited a splendid therapeutic effect in all cases. Further, even though CpG-sEV showed a therapeutic effect to some extent, its therapeutic effect was weaker than that of the CpG-OVA-sEV in an allergic rhinitis mouse model.

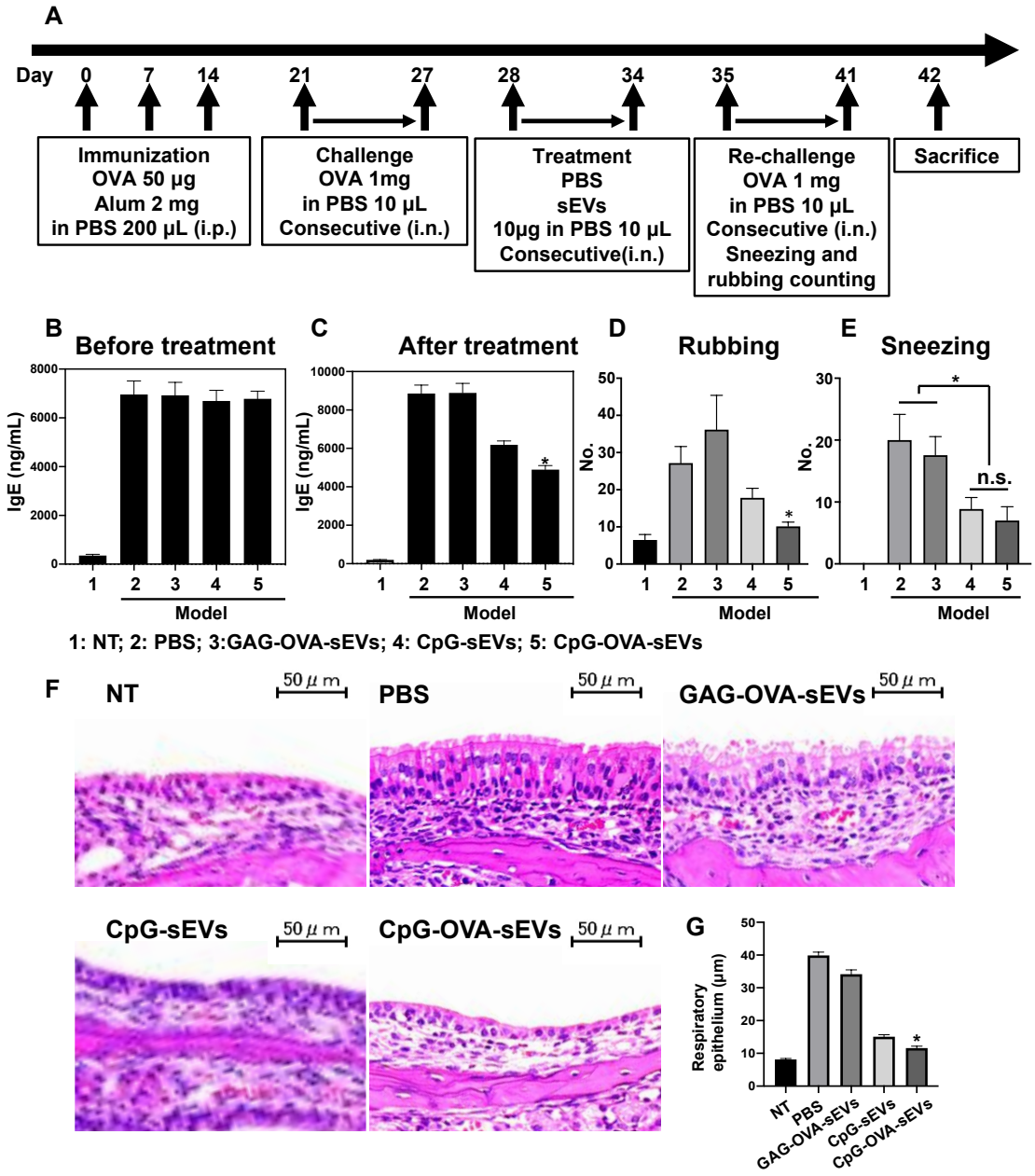

Figure 16. Therapeutic effect of the CpG-OVA-sEVs in the allergic rhinitis mouse model. (A) Immunization and challenge protocol of allergic rhinitis mouse model. (B) IgE concentration of mouse serum on day 27 after the first immunization. (C) IgE concentration of mouse serum on day 42 after the first immunization. (D) Numbers of rubbing and (E) sneezing in 5 min after re-challenge with OVA. (F) Hematoxylin and eosin staining of the mouse nasal mucosa section. (G) The thickness of the respiratory epithelium. *$p < 0.05$ compared with the other groups. The results are expressed as means ± standard error of the mean (NT: n = 4, Model: n = 7).

III-3-f CpG-OVA-sEVs enhanced the Th1 immune response of allergic rhinitis mouse model.

To estimate the OVA-specific Th1 immunostimulatory effect of CpG-OVA-sEVs, spleen cells and serum were collected from the mice on day 42 and restimulated with OVA or BSA. IFN-γ concentrations, as well as IgG1 and IgG2a antibody titers, were measured. Resultantly, the OVA-specific IFN-γ concentration was significantly increased in the CpG-OVA-sEV group (Figure 17A). Moreover, IgG2a, which is an index of the Th1 immune response, was significantly increased in the CpG-OVA-sEV group, while IgG1, an index of the Th2 immune response, was not altered between the mouse model groups, suggesting that the CpG-OVA-sEVs induced a Th1 immune response against OVA (Figures 17B–C).

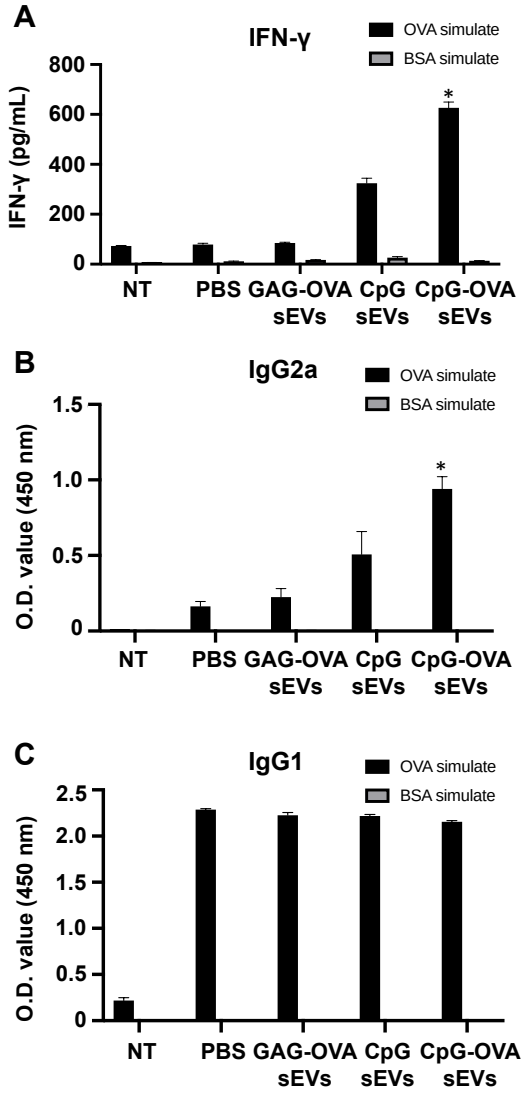

Figure 17. OVA-specific cellular and humoral immunity induced by CpG-OVA-sEV. (A) Spleen cells were co-cultured using an OVA/BSA-coated plate for the cellular immune response, and the concentrations of IFN-γ in the supernatant were detected. (B–C) For the humoral immune response, serum was co-cultured using an OVA/BSA-coated plate. (B) IgG2a and (C) IgG1 titers were detected. *$p < 0.05$ compared with the other groups. The results are expressed as means ± standard error of the mean (NT: n = 4, Model: n = 7).

III-4 Discussion

Since sEVs can encapsulate proteins and nucleic acids derived from the producing cells,

research on cancer immunotherapy utilizing sEVs derived from cancer cells containing endogenous antigens has been actively conducted in recent years[59]. Additionally, exogenous antigens can be loaded onto sEVs by the genetic engineering of the producing cells; however, it is necessary to choose whether to load the antigens onto the outer or inner lipid bilayer of the sEV. Based on the finding in chapter 2 that the loading of antigens on the inner side of sEVs is suitable for the development of immunotherapy using exogenous antigen-loaded sEVs[56], in this chapter, I developed a simultaneous antigen–adjuvant delivery system by modifying CpG DNA on the surface of OVA-encapsulated sEVs. Although there have been other reports on CpG DNA–allergen delivery systems, the dose of CpG DNA was approximately 10–50 μg, and the dose of allergen was approximately 10 μg [60,61]. In this study, a remarkable therapeutic effect was observed at lower doses of CpG DNA (approximately 26 ng) and allergen (100 ng) (Figures 5–6), indicating the usefulness of the sEVs as delivery carriers. Therefore, sEVs are highly desirable antigen–adjuvant vehicles for other purposes, such as vaccines for a variety of diseases.

When administered intranasally, a high dosage volume results in high pulmonary exposure. It has been reported that a total dosage volume of 10 μL has no effect on pulmonary exposure, a dosage volume of 20 μL has a moderate impact, and a dose level of 50 μL or more results in a significant pulmonary exposure[62]. Therefore, to avoid pulmonary exposure, a total dosage volume of 10 μL was selected as the administration dose in this study.

The immune system of the nasal mucosa is called the NALT, which is found on the cartilaginous soft palate of the upper jaw[63]. My immunofluorescence results showed that the CpG-OVA-sEVs were delivered to the NALT, and some of them co-localized with the $CD11c^+$ cells. Although $CD11c^+$ has traditionally been considered a dendritic cell marker, recent studies have found that they are also expressed in some macrophages[64] or B cells[65]. B220 was selected as a B cell marker, and CpG-OVA-sEV showed no co-localization with B220. Therefore, the CpG-OVA-sEVs were taken up by the dendritic cells or macrophages rather than the B cells in the NALT to induce a subsequent immune response.

Because of the therapeutic experiments using allergic rhinitis mice models, the CpG-sEV group showed an anti-allergic effect due to non-specific tolerance. This is consistent with other studies that used CpG DNA as an immunomodulator in an allergen-free formulation[66]. However, the CpG-OVA-sEV group showed a stronger anti-allergic effect than the CpG-sEV group (Figure 5). This is probably because, when CpG DNA is administered in conjunction with an allergen, the resultant tolerance induction is allergen-specific and long-lasting since it

is maintained by immunological memory. Therefore, although therapies using allergen-free CpG DNA seem to produce a certain degree of anti-allergic effects, CpG DNA-based treatment with allergens is preferred and is anticipated to trigger allergen-specific and long-lasting tolerance[67].

CpG DNA has been reported to induce the immune response of Th1 $CD4^+$ T cells, alleviating the symptoms of allergic rhinitis[68]. My antibody titer experiment results shown in Figure 6 showed that the Th1 immune response was enhanced in the CpG-OVA-sEV group. Exogenous antigens are mainly present in $CD4^+$ T cells via MHC class II after being taken up by dendritic cells[69]. However, previous research has demonstrated that antigens loaded in sEVs can also be presented to $CD8^+$ T cells and trigger an immune response by a cross presentation[23,56]. The effector $CD8^+$ T cells have been shown to modulate allergic responses, and CD8-primed $CD11b^+$ $CD103^-$ dendritic cells may bias the differentiation of $CD4^+$ T cells toward a Th1 phenotype[70]. My data in Figure 6 show that IFN-γ levels are elevated in mouse spleen cells that have been restimulated with OVA, and considering that $CD8^+$ T cells may also produce IFN-γ, it is implied that $CD8^+$ T cells may play a non-negligible role in this process.

III-5 Summary of chapter 3

I succeeded in preparing multifunctional sEVs that loaded both antigens (or allergens) and adjuvants. CpG DNA and allergen OVA were simultaneously delivered to dendritic cells, activating dendritic cells *in vitro*. Furthermore, CpG-OVA-sEVs were detected in the NALT after intranasal administration *in vivo*. Finally, I showed that CpG-OVA-sEVs can enhance the Th1 immune response in allergic rhinitis mouse models and alleviate the symptoms of allergic rhinitis. These results prove that multifunctional CpG-OVA-sEVs can be a useful therapeutic method for the treatment of allergic rhinitis.

Conclusion

sEVs are secretory lipid bilayer membrane vesicles with a diameter of around 100 nm, which can function as intercellular transport carriers encapsulating proteins and nucleic acids. sEVs not only contain endogenous antigens derived from secretory cells but can also carry exogenous antigens or functional molecules by genetic engineering. Antigen-loaded multifunctional sEVs are a promising immunotherapy option because of these unique features.

For immunotherapeutic application of sEV, antigen loading, delivery to immune cells (especially dendritic cells, DCs) and activation of the immune cells are important factors. In chapter 1, I successfully developed CD40L modified endogenous antigen-containing multifunctional sEVs, which can be efficiently delivered to DCs and can activate DCs to improve the antigen presentation efficacy of DCs.

To enable the development of new types of multifunctional sEVs, in chapter 2, I attempt to load exogenous antigens into sEVs by using genetic engineering. I found that the localization of antigen proteins loaded in sEVs, inner surface or outer surface, alters the fate of loaded protein in sEV uptake cells. I also found that antigen inner loading sEVs are more suitable to immunotherapy than antigen outer loading sEVs.

In chapter 3, based on the findings of chapter 1 and 2, I modified allergen-loaded sEVs with CpG DNA to develop multifunctional sEVs that can delivery allergen and adjuvant to dendritic cells simultaneously. In allergic rhinitis mouse models, the allergen-loaded multifunctional sEVs showed a significant therapeutic effect.

The findings in this thesis contribute to the development of antigen-loaded multifunctional sEVs-based immunotherapies.

List of publications included in this thesis

Development of CD40L-modified tumor small extracellular vesicles for the effective induction of anti-tumor immune response.

Nanomedicine (Lond). (2020) **15**:1641 ~ 1652

Effects of localization of antigen proteins in antigen-loaded exosomes on efficiency of antigen presentation.

Molecular Pharmaceutics. (2019) **16**:2309 ~ 2314

Development of allergic rhinitis immunotherapy using antigen-loaded multifunctional small extracellular vesicles.

Submitted

Acknowledgments

First and foremost, I would like to express my gratitude to Professor Yoshinobu Takakura, Ph.D. from the Department of Biopharmaceutics and Drug Metabolism, Graduate School of Pharmaceutical Sciences, Kyoto University for accepting me as his student and giving me the opportunity to come to Japan to meet so many wonderful people in his lab. I would like to thank him for his patient guidance, and warm encouragements, which enabled me to progress swiftly over the course of five and a half years to get my Ph.D. degree.

Then, as my direct supervisor, I would like to express my gratitude to Associate Professor Yuki Takahashi, Ph.D. from the Department of Biopharmaceutics and Drug Metabolism, for his patient assistance and advice. In addition to research, since I was new to Japan and my Japanese was not very excellent at the time, Dr. Takahashi also coached me a lot in academic Japanese. Under Dr. Takahashi's instruction, I learned how to undertake independent research and solve difficulties. I would not have been able to complete my Ph.D. course without his assistance.

I would like to extend my sincere thanks to Professor Makiya Nishikawa, Ph.D. from Laboratory of Biopharmaceutics, Faculty of Pharmaceutical Sciences, Tokyo University of Science, for his insightful comments, and suggestions in chapter 1 and 2.

I would like to thank Assistant Professor Yusuke Kawamoto, Ph.D. from the Department of Biopharmaceutics and Drug Metabolism, and Assistant Professor Masaki Morishita, Ph.D. from the Department of Biopharmaceutics, Kyoto Pharmaceutical University, for their valuable discussion and kind support.

I would like to thank all members of the Department of Biopharmaceutics and Drug Metabolism, both the alumni and current members, for their help with life and experiments, as well as the lovely memories we have had over the past five and a half years. I would like to give my special thanks to Ms. Noriko Hikihara, Dr. Charoenviriyakul Chonlada, Dr. Akihiro Matsumoto, Mr. Reiichi Ariizumi, Mr. Yuta Arima, Mr. Keisuke Umemura, Ms. Misako Takenaka, Ms. Maki Ota, Ms. Mayu Tabushi for the unstinting help.

I would like to thank the Kobayashi Foundation for financial support (Special Research Fellowship for international students), for helping me with general advice and guidance on living in Japan.

Many thanks for my dear roommate, Dr. Tianqi Zhang. Thank you for your ten years of

friendship and support, as well as all the advice and assistance you've provided me throughout my life and research.

Last but not least, I would like to express my gratitude to my family (grandmothers, parents, aunts) for raising me and educating me to be a responsible adult capable of facing the world alone and boldly. Thank you for providing me with a decent education that enabled me to study abroad, travel the globe, and pursue my aspirations. I can be fearless and go forward bravely because of your love and support.

Reference

1 Tkach M, Théry C. Communication by Extracellular Vesicles: Where We Are and Where We Need to Go. *Cell* 164(6), 1226–1232 (2016).

2 An Q, Ehlers K, Kogel K, Bel AJEV, Hückelhoven R. Multivesicular compartments proliferate in susceptible and resistant MLA12-barley leaves in response to infection by the biotrophic powdery mildew fungus. *New Phytol* 172(3), 563–576 (2006).

3 Sánchez C, Franco L, Regal P, Lamas A, Cepeda A, Fente C. Breast Milk: A Source of Functional Compounds with Potential Application in Nutrition and Therapy. *Nutrients* 13(3), 1026 (2021).

4 Wang L, Liu T, Chen G *et al.* Exosomal microRNA let-7-5p from Taenia pisiformis Cysticercus Prompted Macrophage to M2 Polarization through Inhibiting the Expression of C/EBP δ. *Microorg* 9(7), 1403 (2021).

5 Johnstone RM, Bianchini A, Teng K. Reticulocyte maturation and exosome release: transferrin receptor containing exosomes shows multiple plasma membrane functions. *Blood* 74(5), 1844–51 (1989).

6 Valadi H, Ekström K, Bossios A, Sjöstrand M, Lee JJ, Lötvall JO. Exosome-mediated transfer of mRNAs and microRNAs is a novel mechanism of genetic exchange between cells. *Nat Cell Biol* 9(6), 654–659 (2007).

7 Crescitelli R, Lässer C, Lötvall J. Isolation and characterization of extracellular vesicle subpopulations from tissues. *Nat Protoc* 16(3), 1548–1580 (2021).

8 Théry C, Witwer KW, Aikawa E *et al.* Minimal information for studies of extracellular vesicles 2018 (MISEV2018): a position statement of the International Society for Extracellular Vesicles and update of the MISEV2014 guidelines. *J Extracell Vesicles* 8(1), 1535750 (2018).

9 Kowal J, Tkach M, Théry C. Biogenesis and secretion of exosomes. *Curr Opin Cell Biol* 29, 116–125 (2014).

10 Niel G van, D'Angelo G, Raposo G. Shedding light on the cell biology of extracellular vesicles. *Nat Rev Mol Cell Bio* 19(4), 213–228 (2018).

11 Shah S, Dhawan V, Holm R, Nagarsenker MS, Perrie Y. Liposomes: Advancements and innovation in the manufacturing process. *Adv Drug Deliver Rev* 154–155, 102–122 (2020).

12 Sheoran R, Khokra SL, Chawla V, Dureja H. Recent Patents, Formulation Techniques, Classification and Characterization of Liposomes. *Recent Pat Nanotech* 13(1), 17–27 (2019).

13 Xu M, Yang Q, Sun X, Wang Y. Recent Advancements in the Loading and Modification of

Therapeutic Exosomes. *Frontiers Bioeng Biotechnology* 8, 586130 (2020).

14 Wolfers J, Lozier A, Raposo G *et al.* Tumor-derived exosomes are a source of shared tumorrejection antigens for CTL cross-priming. *Nat. Med.* VOLUME 7(NUMBER 3) (2001).

15 Yamashita T, Takahashi Y, Takakura Y. Possibility of Exosome-Based Therapeutics and Challenges in Production of Exosomes Eligible for Therapeutic Application. *Biological Pharm Bulletin* 41(6), 835–842 (2018).

16 Bae S, Brumbaugh J, Bonavida B. Exosomes derived from cancerous and non-cancerous cells regulate the anti-tumor response in the tumor microenvironment. *Genes Cancer* 9(3–4), 87–100 (2018).

17 Segura E, Villadangos JA. Antigen presentation by dendritic cells in vivo. *Curr Opin Immunol* 21(1), 105–110 (2009).

18 Gutiérrez-Martínez E, Planès R, Anselmi G *et al.* Cross-Presentation of Cell-Associated Antigens by MHC Class I in Dendritic Cell Subsets. *Front Immunol* 6, 363 (2015).

19 Yin W, Gorvel L, Zurawski S *et al.* Functional Specialty of CD40 and Dendritic Cell Surface Lectins for Exogenous Antigen Presentation to CD8+ and CD4+ T Cells. *Ebiomedicine* 5(Proc. Natl. Acad. Sci. U. S. A. 106 2009), 46–58 (2016).

20 Cruz LJ, Rosalia RA, Kleinovink JW, Rueda F, Löwik CWGM, Ossendorp F. Targeting nanoparticles to CD40, DEC-205 or CD11c molecules on dendritic cells for efficient CD8+ T cell response: A comparative study. *J Control Release* 192(Nat. Immunol. 3 2002), 209–218 (2014).

21 Grewal IS, Flavell RA. CD40 and CD154 in cell-mediated immunity. *Annu. Rev. Immunol.* 16, 111–35 (1998).

22 Karnell JL, Rieder SA, Ettinger R, Kolbeck R. Targeting the CD40-CD40L pathway in autoimmune diseases: Humoral immunity and beyond. *Adv Drug Deliver Rev* (Immunol. Rev. 229 1 2009) (2018).

23 Embgenbroich M, Burgdorf S. Current Concepts of Antigen Cross-Presentation. *Front Immunol* 9, 1643 (2018).

24 Cafri G, Sharbi-Yunger A, Tzehoval E, Eisenbach L. Production of LacZ Inducible T Cell Hybridoma Specific for Human and Mouse gp10025–33 Peptides. *Plos One* 8(2), e55583 (2013).

25 Takahashi Y, Nishikawa M, Shinotsuka H *et al.* Visualization and in vivo tracking of the exosomes of murine melanoma B16-BL6 cells in mice after intravenous injection. *J Biotechnol* 165(2), 77–84 (2013).

26 Morishita M, Takahashi Y, Matsumoto A, Nishikawa M, Takakura Y. Exosome-based tumor antigens–adjuvant co-delivery utilizing genetically engineered tumor cell-derived exosomes with immunostimulatory CpG DNA. *Biomaterials* 111, 55–65 (2016).

27 Yamashita T, Takahashi Y, Nishikawa M, Takakura Y. Effect of exosome isolation methods on physicochemical properties of exosomes and clearance of exosomes from the blood circulation. *Eur J Pharm Biopharm* 98, 1–8 (2016).

28 Inaba K, Inaba M, Romani N *et al.* Generation of Large Numbers of Dendritic Cells from Mouse Bone Marrow Cultures Supplemented with Granulocyte/Macrophage Colony-stimulating Factor. *J. Exp. Med.* 176, 1693–1702 (1992).

29 Apostolopoulos V, Thalhammer T, Tzakos AG, Stojanovska L. Targeting Antigens to Dendritic Cell Receptors for Vaccine Development. *J Drug Deliv* 2013, 1–22 (2013).

30 Takahashi Y, Nishikawa M, Takakura Y. In Vivo Tracking of Extracellular Vesicles in Mice Using Fusion Protein Comprising Lactadherin and Gaussia Luciferase. In: (*Volume 1660*). Kuo" ["Winston Patrick, Jia"] "Shidong (Ed.), Springer New York, New York, NY, 245–254 (2017).

31 Chatterjee B, Smed-Sörensen A, Cohn L *et al.* Internalization and endosomal degradation of receptor-bound antigens regulate the efficiency of cross presentation by human dendritic cells. *Blood* 120(10), 2011–2020 (2012).

32 Chen Y, Chen J, Xiong Y *et al.* Internalization of CD40 regulates its signal transduction in vascular endothelial cells. *Biochem Bioph Res Co* 345(1), 106–117 (2006).

33 Tai Y-T, Catley LP, Mitsiades CS *et al.* Mechanisms by which SGN-40, a Humanized Anti-CD40 Antibody, Induces Cytotoxicity in Human Multiple Myeloma Cells: Clinical Implications. *Cancer Res.* (64), 2846–2852 (2015).

34 Kou L, Sun J, Zhai Y, He Z. The endocytosis and intracellular fate of nanomedicines: Implication for rational design. *Asian J Pharm Sci* 8(1), 1–10 (2013).

35 Schuette V, Burgdorf S. The ins-and-outs of endosomal antigens for cross-presentation. *Curr Opin Immunol* 26, 63–68 (2014).

36 Manning E, Pullen SS, Souza DJ, Kehry M, Noelle RJ. Cellular responses to murine CD40 in a mouse B cell line may be TRAF dependent or independent. *Eur J Immunol* 32(1), 39–49 (2002).

37 Marigo I, Zilio S, Desantis G *et al.* T Cell Cancer Therapy Requires CD40-CD40L Activation of Tumor Necrosis Factor and Inducible Nitric-Oxide-Synthase-Producing Dendritic Cells. *Cancer Cell* 30(3), 377–390 (2016).

38 Dakal TC, Dhabhai B, Agarwal D *et al.* Mechanistic basis of co-stimulatory CD40-CD40L ligation mediated regulation of immune responses in cancer and autoimmune disorders. *Immunobiology* 151899 (2019).

39 Bowen WS, Svrivastava AK, Batra L, Barsoumian H, Shirwan H. Current challenges for cancer vaccine adjuvant development. *Expert Rev Vaccines* 17(3), 207–215 (2018).

40 Charoenviriyakul C, Takahashi Y, Morishita M, Nishikawa M, Takakura Y. Role of extracellular vesicle surface proteins in the pharmacokinetics of extracellular vesicles. *Mol Pharmaceut* (2018).

41 Mulcahy LA, Pink RC, Carter DRF. Routes and mechanisms of extracellular vesicle uptake. *J Extracell Vesicles* 3(1), 24641 (2014).

42 Savina A, Peres A, Cebrian I *et al.* The Small GTPase Rac2 Controls Phagosomal Alkalinization and Antigen Crosspresentation Selectively in CD8+ Dendritic Cells. *Immunity* 30(4), 544–555 (2009).

43 Gao J, Ochyl LJ, Yang E, Moon JJ. Cationic liposomes promote antigen cross-presentation in dendritic cells by alkalizing the lysosomal pH and limiting the degradation of antigens. *Int J Nanomed* 12, 1251–1264 (2017).

44 Bousquet J, Anto JM, Bachert C *et al.* Allergic rhinitis. *Nat Rev Dis Primers* 6(1), 95 (2020).

45 Bousquet P -J., Leynaert B, Neukirch F *et al.* Geographical distribution of atopic rhinitis in the European Community Respiratory Health Survey I*. *Allergy* 63(10), 1301–1309 (2008).

46 Hossenbaccus L, Linton S, Garvey S, Ellis AK. Towards definitive management of allergic rhinitis: best use of new and established therapies. *Allergy Asthma Clin Immunol* 16(1), 39 (2020).

47 Meng Y, Wang C, Zhang L. Advances and novel developments in allergic rhinitis. *Allergy* 75(12), 3069–3076 (2020).

48 Senna G, Ridolo E, Calderon M, Lombardi C, Canonica GW, Passalacqua G. Evidence of adherence to allergen-specific immunotherapy. *Curr Opin Allergy Cl* 9(6), 544–548 (2009).

49 Klinman DM. Immunotherapeutic uses of CpG oligodeoxynucleotides. *Nat Rev Immunol* 4(4), 249–259 (2004).

50 Ishii-Mizuno Y, Umeki Y, Takahashi Y *et al.* Nasal delivery of Japanese cedar pollen Cryj1 by using self-gelling immunostimulatory DNA for effective induction of immune responses in mice. *J Control Release* 200, 52–59 (2015).

51 Fukuiwa T, Sekine S, Kobayashi R *et al.* A combination of Flt3 ligand cDNA and CpG ODN as nasal adjuvant elicits NALT dendritic cells for prolonged mucosal immunity. *Vaccine* 26(37),

4849–4859 (2008).

52 Hessenberger M, Weiss R, Weinberger EE, Boehler C, Thalhamer J, Scheiblhofer S. Transcutaneous delivery of CpG-adjuvanted allergen via laser-generated micropores. *Vaccine* 31(34), 3427–3434 (2013).

53 Klimek L, Willers J, Hammann-Haenni A *et al.* Assessment of clinical efficacy of CYT003-QbG10 in patients with allergic rhinoconjunctivitis: a phase IIb study. *Clin Exp Allergy* 41(9), 1305–1312 (2011).

54 Kalluri R, LeBleu VS. The biology, function, and biomedical applications of exosomes. *Science* 367(6478), eaau6977 (2020).

55 Herrmann IK, Wood MJA, Fuhrmann G. Extracellular vesicles as a next-generation drug delivery platform. *Nat Nanotechnol* 16(7), 748–759 (2021).

56 Arima Y, Liu W, Takahashi Y, Nishikawa M, Takakura Y. Effects of localization of antigen proteins in antigen-loaded exosomes on efficiency of antigen presentation. *Mol Pharmaceut* (2019).

57 Morishita M, Takahashi Y, Nishikawa M *et al.* Quantitative Analysis of Tissue Distribution of the B16BL6-Derived Exosomes Using a Streptavidin–Lactadherin Fusion Protein and Iodine-125-Labeled Biotin Derivative After Intravenous Injection in Mice. *J Pharm Sci* 104(2), 705–713 (2015).

58 Vieira GC, Gadelha FAAF, Pereira RF *et al.* Warifteine, an alkaloid of Cissampelos sympodialis, modulates allergic profile in a chronic allergic rhinitis model. *Revista Brasileira De Farmacognosia* 28(1), 50–56 (2018).

59 Tai Y-L, Chu P-Y, Lee B-H *et al.* Basics and applications of tumor-derived extracellular vesicles. *J Biomed Sci* 26(1), 35 (2019).

60 Suzuki M, Matsumoto T, Ohta N, Min W-P, Murakami S. Intranasal CpG DNA therapy during allergen exposure in allergic rhinitis. *Otolaryngology- Head Neck Surg* 136(2), 246–251 (2007).

61 Ashino S, Wakita D, Zhang Y, Chamoto K, Kitamura H, Nishimura T. CpG-ODN inhibits airway inflammation at effector phase through down-regulation of antigen-specific Th2-cell migration into lung. *Int Immunol* 20(2), 259–266 (2008).

62 Miller MA, Stabenow JM, Parvathareddy J *et al.* Visualization of Murine Intranasal Dosing Efficiency Using Luminescent Francisella tularensis: Effect of Instillation Volume and Form of Anesthesia. *Plos One* 7(2), e31359 (2012).

63 Cisney ED, Fernandez S, Hall SI, Krietz GA, Ulrich RG. Examining the Role of

Nasopharyngeal-associated Lymphoreticular Tissue (NALT) in Mouse Responses to Vaccines. *J Vis Exp Jove* (66), 3960 (2012).

64 Zhu Y, Zhang L, Lu Q *et al.* Identification of different macrophage subpopulations with distinct activities in a mouse model of oxygen-induced retinopathy. *Int J Mol Med* 40(2), 281–292 (2017).

65 Golinski M-L, Demeules M, Derambure C *et al.* CD11c+ B Cells Are Mainly Memory Cells, Precursors of Antibody Secreting Cells in Healthy Donors. *Front Immunol* 11, 32 (2020).

66 Sabatel C, Radermecker C, Fievez L *et al.* Exposure to Bacterial CpG DNA Protects from Airway Allergic Inflammation by Expanding Regulatory Lung Interstitial Macrophages. *Immunity* 46(3), 457–473 (2017).

67 Montamat G, Leonard C, Poli A, Klimek L, Ollert M. CpG Adjuvant in Allergen-Specific Immunotherapy: Finding the Sweet Spot for the Induction of Immune Tolerance. *Front Immunol* 12, 590054 (2021).

68 Farrokhi S, Abbasirad N, Movahed A, Khazaei HA, Pishjoo M, Rezaei N. TLR9-based immunotherapy for the treatment of allergic diseases. *Immunotherapy* 9(4), 339–346 (2017).

69 Neefjes J, Jongsma MLM, Paul P, Bakke O. Towards a systems understanding of MHC class I and MHC class II antigen presentation. *Nat Rev Immunol* 11(12), 823–836 (2011).

70 Tang Y, Guan SP, Chua BYL *et al.* Antigen-specific effector CD8 T cells regulate allergic responses via IFN-γ and dendritic cell function. *J Allergy Clin Immun* 129(6), 1611-1620.e4 (2012).